Disentangling Brazilian TFP: the role of misallocation in recent economic cycles

Tomás R. Martinez
Insper
tomas.martinez@insper.edu.br

Thiago Trafane Oliveira Santos
Banco Central do Brasil
thiago.trafane@bcb.gov.br

Abstract

This paper investigates the role of market-power-driven misallocation in shaping TFP during recent economic cycles in Brazil, using the static Cournot model of Martinez and Santos (2024). The model primarily relies on macroeconomic data for calibration, allowing us to decompose Brazil's national TFP into technology and allocative efficiency components from 2000 to 2019. Over these two decades, we observe an upward trend in allocative efficiency, reflecting an increase in the labor income share and a corresponding decrease in the average markup, in sharp contrast with most developed countries. Our results further indicate that the cycles in Brazilian TFP are largely driven by allocative efficiency, with the mid-2000s economic boom mainly attributed to efficiency gains. In contrast, the technology component grows more steadily, around 0.9% per year, suggesting it reflects structural characteristics of the economy. Since allocative efficiency is bounded, this 0.9% annual growth rate can be interpreted as the current long-run growth level of TFP in Brazil.

JEL codes: L11, L13, O47, O54.
Keywords: TFP, misallocation, Cournot model, Brazil.

1 Introduction

Economic growth is often shaped by the behavior of total factor productivity (TFP) (e.g., Jones 2016, Bergeaud et al. 2018, and Crafts and Woltjer 2021). In Brazil, the story is no different, with the economic boom in the mid-2000s driven by rapid gains in TFP. The challenge lies in understanding TFP, which is notoriously difficult. On the one hand, from an empirical perspective, TFP is a residual, "a measure of our ignorance," capturing the portion of output (e.g., GDP) that cannot be explained by the measured inputs (e.g., labor and capital). As a residual, the drivers of TFP are, by construction, unknown. On the other hand, from a theoretical perspective, there are so many potential determinants of TFP that arriving at a definitive answer is practically impossible. Broadly speaking, a country's TFP grows when (i) firms' productivity improves, or (ii) resources become better allocated across firms. However, as discussed by Syverson (2011), the determinants of firm-level productivity are numerous, ranging from internal factors (e.g., managerial practices, R&D, and learning-by-doing) to external ones (e.g., productivity spillovers, competition, and regulation). Similarly, many factors lead to resource misallocation, including taxes, regulations, subsidized credit, corruption, and market frictions (see Restuccia and Rogerson 2013 for a survey of this literature).

In this paper, we investigate the role of market-power-driven misallocation in shaping Brazilian TFP across recent economic cycles. Specifically, we apply the static Cournot model of Martinez and Santos (2024) to decompose Brazilian TFP into technology and allocative efficiency components from 2000 to 2019. In their model, firms produce a homogeneous good and are heterogeneous in productivity, with a large number of inefficient firms due to free entry among low-productivity firms. As firms compete à la Cournot, the differences in productivity lead to heterogeneous markups, resulting in misallocation as marginal products are not equalized across firms. A novel feature of this model is its primary reliance on macroeconomic data for calibration, which stems from the stronger underlying assumptions (e.g., homogeneous goods and free entry among low-productivity firms). This is exactly what allows us to decompose Brazil's national TFP over two decades.

In calibrating the model, Martinez and Santos (2024) assume firm productivity follows a truncated Pareto distribution, testing various values for the Pareto shape parameter and identifying the distributional support by matching the aggregate TFP and the cost-weighted average of firm-level markups. We adopt a similar approach but go further by estimating the shape parameter, targeting a measure of concentration: the number of active firms multiplied by the Herfindahl–Hirschman index (HHI) of the labor market.

To compute the target moments using real-world data, we first parameterize the firms' production function, which is Cobb-Douglas with constant returns to scale, using both capital and labor as inputs. The capital share parameter, α, is calibrated to 0.39 based on cost share data. Labor expenses are sourced directly from the National Accounts, while capital expenses are calculated following Barkai (2020), estimating a required rate of return in the spirit of Hall and

Jorgenson (1967). With α determined, the first two moments are straightforward to obtain from standard macroeconomic data. The cost-weighted average markup is equal to $1 - \alpha$ divided by the labor share of national income, while TFP is backed out as a residual from the aggregate production function. Naturally, obtaining this last moment requires data on labor and capital stock, which are both adjusted for input usage based on a capacity utilization survey. Rather than merely multiplying the capital stock by a capacity utilization indicator, we introduce a "capacity utilization share parameter." This imposes capital and labor utilization is simply a rescaling of an observable measure of input usage intensity, in line with Basu et al. (2006) and Basu et al. (2013). To estimate this share parameter, we rely on the dynamic panel literature on production function estimation (e.g., Blundell and Bond 2000). Specifically, we use the simplified version of these methods presented in Ackerberg et al. (2015), but apply it to time series rather than panel data.

However, obtaining a representative third moment for the entire economy proves challenging even with comprehensive firm-level data, as it involves the complex task of defining the relevant market for each firm in the economy (see Berry et al. 2019, Syverson 2019, and Benkard et al. 2021 for a discussion). Given this difficulty, we pursue a weaker moment match in this case, trying only to approximate the shape of its time series by targeting the moment normalized. This approach avoids the need for precise estimation of this data moment, as both its mean and variance become irrelevant, allowing us to rely on relatively aggregate employment data and simple assumptions about the relevant markets (e.g., a single national market).

Turning to our empirical results, we observe an upward trend in allocative efficiency between 2000 and 2019. This reflects the observed increase in the labor income share and, thus, the estimated decrease in the average markup, as misallocation increases with the average markup in the model (Martinez and Santos 2024). This contrasts sharply with most developed countries, which have experienced a decreasing labor share and increasing average markup over the last decades (e.g., Calligaris et al. 2018, De Loecker and Eeckhout 2018, and Autor et al. 2020). Accordingly, Baqaee and Farhi (2020) find the distance from optimal allocation widened in 2015 compared to 1997 in the US. Additionally, our results show that the cycles in Brazilian TFP are largely driven by allocative efficiency, with the economic boom in the mid-2000s primarily attributed to efficiency gains. In contrast, the technology component of TFP grows more steadily, around 0.9% per year, suggesting it reflects structural characteristics of the economy. Since allocative efficiency is bounded and consequently cannot increase or decrease indefinitely, this 0.9% annual growth rate can be interpreted as the current long-run growth level of Brazilian TFP.

We demonstrate our main conclusions hold across four robustness exercises. First, we re-estimate the model assuming a uniform distribution of productivity, using *only* macroeconomic data for calibration, as the third moment is not required in this case.[1] According to Martinez

[1]This makes the model robust to potential measurement errors in labor market concentration data. Our primary quantification strategy only requires sound estimates of overall trends in labor market concentration. However, even

and Santos (2024), this effectively selects the Pareto shape parameter that leads to the most conservative reasonable TFP decomposition compared to standard accounting exercises, where all TFP variation is attributed to technology. Second, we set the capital share parameter α to the standard value of 1/3 or to 0.41, instead of our baseline calibration ($\alpha = 0.39$). Third, we experiment with a higher labor income share by allocating all self-employment income (mixed income) to labor. In the baseline case, mixed income is allocated to labor and non-labor in the same proportions as the rest of the economy, following the preferred method of the Penn World Table 10.01 (Feenstra et al. 2015). Finally, instead of selecting a productivity density, we impose a firm market share distribution that is consistent with empirical evidence supporting Zipf's law for firm size (Okuyama et al. 1999, Axtell 2001, Fujiwara et al. 2004, Luttmer 2007, Gabaix and Landier 2008, Di Giovanni et al. 2011, Di Giovanni and Levchenko 2013, Da Silva et al. 2018, and Santos and Cajueiro 2024). We search for the distributional parameters by matching the model's predictions to the same three data moments used in the baseline case.

Related literature. We employ the static Cournot model of Martinez and Santos (2024), which relates to several papers that embed oligopoly market structures in macroeconomic models (e.g., Bernard et al. 2003, Atkeson and Burstein 2008, Edmond et al. 2015, Peters 2020, De Loecker et al. 2021, Wang and Werning 2022, and Edmond et al. 2022). Their model is notable for requiring minimal microdata for calibration, achieved through reliance on stronger assumptions. We contribute to their work in several dimensions. First, we derive the model's expressions for (i) the HHI of the labor market and (ii) the HHI of the product market. Second, using that expression for labor market concentration, we estimate the Pareto shape parameter using real-world data, whereas Martinez and Santos (2024) explore scenarios by assigning different values to the shape parameter. Third, in a robustness exercise, we extend the analysis beyond a Pareto productivity density and assume firm market share follows a Lomax distribution. Martinez and Santos (2024) establish necessary and sufficient conditions for achieving an exact match of the first two target moments, namely, aggregate TFP and average markup. They first derive general results by examining an arbitrary truncated distribution, which they subsequently apply to delineate the specific conditions for the Pareto case. We adopt a similar strategy, utilizing their general results to derive analogous conditions for the Lomax case. Finally, we account for the potential underutilization of inputs and adjust capital and labor using a capacity utilization survey, in the spirit of Basu et al. (2006) and Basu et al. (2013).

Given our goal of disentangling TFP growth, this paper is closely related to the growth-accounting literature and its various methodologies for decomposing TFP into technology and allocative efficiency components (e.g., Basu and Fernald 2002, Petrin and Levinsohn 2012, and Baqaee and Farhi 2020). Despite their differences, all these methods rely on highly general

this requirement may not always be met. For instance, Benkard et al. (2021) calculate product market concentration in the US from 1994 to 2019 for (i) "narrowly defined product markets as would be defined in an antitrust setting" (Benkard et al. 2021, p.1) and (ii) broader sector levels (similar to our approach), finding decreasing concentration in the first case but increasing in the second.

models that do not impose any specific market structure but require extensive microdata, which are hardly available for all firms in the economy. The common solution is to use (i) sectoral data that span the entire economy (e.g., Basu and Fernald 2002), (ii) firm-level data that do not span the economy (e.g., Petrin and Levinsohn 2012), or (iii) a combination of both (e.g., Baqaee and Farhi 2020). We follow an alternative approach, employing the model of Martinez and Santos (2024), which requires minimal microdata by relying on stronger model assumptions. Another difference is that Martinez and Santos (2024) measure allocative efficiency by the distance from optimal allocation, which contrasts with the concept typically adopted in this literature. As Baqaee and Farhi (2020, p.107) point out, "the growth-accounting notion of changes in allocative efficiency due to the reallocation of resources to more or less distorted parts of the economy over time is very different from the misallocation literature's notion of allocative efficiency measured as the distance to the Pareto-efficient frontier."

Finally, our work shares common ground with the literature on misallocation (see, e.g., Restuccia and Rogerson 2008, Hsieh and Klenow 2009, and the survey article by Restuccia and Rogerson 2013).[2] However, in this literature, misallocation results from exogenous wedges, whose estimation requires extensive firm-level data, similar to growth-accounting methods. In contrast, in the model of Martinez and Santos (2024), misallocation is endogenous, emerging as an equilibrium outcome. Moreover, the typical goal in this literature is to assess the importance of misallocation in explaining cross-country TFP differences, often within the manufacturing sector due to data availability, whereas we focus on economy-wide TFP evolution over time within a single country.

The remainder of the paper is organized as follows. Section 2 briefly reviews the model of Martinez and Santos (2024). Section 3 outlines our quantification strategy, which requires data and parameters obtained in Section 4. Section 5 presents the baseline empirical results, while Section 6 conducts robustness checks. Finally, Section 7 offers concluding remarks.

2 Model

We use the static Cournot model of Martinez and Santos (2024), where firms have different productivity levels and consequently charge distinct markups, leading to the misallocation of resources. Formally, in a closed economy, N potential entrant firms produce a single good. The price elasticity of demand for this good is strictly negative, with its absolute value denoted by η, where $1 < \eta < \infty$. The output of firm $i \in \{1, 2, ..., N\}$ is given by the Cobb-Douglas function

$$Y_i = A_i K_i^{\alpha} L_i^{1-\alpha}, \tag{1}$$

[2]For studies on misallocation in Brazil, see Busso et al. (2013), Vasconcelos (2017), and Calice et al. (2018) for manufacturing, and De Vries (2014) for the retail sector.

where $K_i \geq 0$ is the capital stock, $L_i \geq 0$ is the labor employed, and $A_i > 0$ is a productivity parameter, all for firm i, with $\alpha \in (0,1)$. Let $\underline{\underline{A}} \equiv \min_i\{A_i\}$ and $\overline{A} \equiv \max_i\{A_i\}$ be the technology frontier of this economy, with $0 < \underline{\underline{A}} < \overline{A} < +\infty$. Denote the empirical probability of A by $g(A)$ and the corresponding empirical cumulative distribution function by $G(A) = \sum_{a<A} g(a)$.

These firms compete à la Cournot, each taking the wage $w > 0$ and the rental cost of capital $r > 0$ as given. There are no fixed costs, but some firms may not be active due to the assumption of homogeneous goods. As a result, Martinez and Santos (2024) employ an entry stage to determine the set of active firms in equilibrium, when (i) each active firm earns non-negative profits and (ii) non-active firms would incur strictly negative profits if they entered the market. However, this equilibrium is typically not unique (Atkeson and Burstein 2008, Edmond et al. 2015, De Loecker et al. 2021). To avoid multiple equilibria, they discard any equilibrium where a non-active firm has a lower marginal cost than an active firm. Consequently, in the (unique) refined equilibrium, there is a firm with productivity $\underline{A}$ that serves as the cutoff for active firms, such that firm i is active if and only if $A_i \geq \underline{A}$. Finally, they consider free entry among low-productivity firms, supposing the number of such firms is sufficiently large to the extent that some should be inactive. This implies the profit of a firm with productivity $\underline{A}$ should be, in some sense, low. Martinez and Santos (2024) assume it is approximately zero.

Given this setup, they show

$$s(A_i) \approx \eta \left(1 - \underline{A}/A_i\right), \tag{2}$$

where $s(A_i)$ is the market share of a firm with productivity A_i, $A_i \geq \underline{A}$. Clearly, more productive firms have higher market shares and, consequently, higher profits, given that all firms charge the same price (homogeneous goods) and that (constant) marginal cost strictly decreases with productivity. Moreover, the marginal active firm, whose productivity is $\underline{A}$, has roughly zero output and profit, as expected. Interestingly, the demand elasticity η can be inferred from the empirical distribution of productivity among active firms:

$$\eta \approx \frac{1}{N_a \left[1 - \mathrm{E}_a\left(\underline{A}/A\right)\right]}, \tag{3}$$

with $\mathrm{E}_a\left(h(A)\right) \equiv \mathrm{E}\left(h(A) | A \geq \underline{A}\right) = \sum_{A \geq \underline{A}} h(A) \frac{g(A)}{1-G(\underline{A})}$ being the expected value of a function h over active firms under the empirical distribution, and $N_a \equiv N\left(1 - G(\underline{A})\right)$ being the number of active firms.

They use these results to derive the aggregate production function. Let $Y \equiv \sum_{i=1}^{N} Y_i$ be the aggregate output, $K \equiv \sum_{i=1}^{N} K_i$ be the aggregate capital stock, and $L \equiv \sum_{i=1}^{N} L_i$ be the aggregate amount of labor employed. They obtain the following aggregate Cobb-Douglas

production function:

$$Y = \overline{A}\Omega K^{\alpha} L^{1-\alpha}, \tag{4}$$

where $\overline{A}\Omega$ represents the aggregate TFP, which comprises two components. First, the efficient TFP level $\overline{A}$, as the homogeneity of goods implies that the optimal allocation entails assigning all inputs to the most productive firm, which has productivity $\overline{A}$. Second, the allocative efficiency $\Omega \in (0, 1]$, measuring the distance of aggregate TFP, $\overline{A}\Omega$, from its optimal level, $\overline{A}$, where

$$\Omega \approx \frac{\mathrm{E}_a\left[(\underline{A}/\overline{A})(1 - \underline{A}/A)\right]}{\mathrm{E}_a\left[(\underline{A}/A)(1 - \underline{A}/A)\right]}. \tag{5}$$

Martinez and Santos (2024) show Ω improves as $\underline{A}$ increases due to the exit of less productive active firms, suggesting higher productivity dispersion among active firms is associated with worse allocative efficiency. In particular, since any allocation of resources is optimal in the absence of productivity heterogeneity, they demonstrate $\Omega \to 1$ as $\underline{A} \to \overline{A}$, which resembles a market in perfect competition, where all active firms have unitary markups and zero profits, with $N_a \to \infty$.

The empirical strategy proposed in Martinez and Santos (2024) relies on the cost-weighted average of firm-level markups, defined as $\mu \equiv \sum_{i=1}^{N} \left(\frac{L_i w + K_i r}{Lw + Kr}\right) \mu_i$, where μ_i denotes the markup of firm i. Specifically, they show

$$\mu \approx \frac{\overline{A}\Omega}{\underline{A}}. \tag{6}$$

Using their results, we derive expressions for two measures of concentration: (i) the Herfindahl–Hirschman index (HHI) of the labor market $HHI_L \equiv \sum_{i=1}^{N} (L_i/L)^2$ and (ii) the HHI of the product market $HHI_s \equiv \sum_{i=1}^{N} s(A_i)^2$. As shown in Appendix A,

$$N_a HHI_L \approx \frac{\mathrm{E}_a\left[(\underline{A}/A)^2 \left(1 - \underline{A}/A\right)^2\right]}{\left\{\mathrm{E}_a\left[(\underline{A}/A)(1 - \underline{A}/A)\right]\right\}^2} \tag{7}$$

$$N_a HHI_s \approx \frac{\mathrm{E}_a\left[(1 - \underline{A}/A)^2\right]}{\left[\mathrm{E}_a\left(1 - \underline{A}/A\right)\right]^2} \approx \frac{1 - 1/\mu}{1 - \mathrm{E}_a\left(\underline{A}/A\right)}. \tag{8}$$

Martinez and Santos (2024) also present a version of the model with a continuum of firms of mass N. However, unlike the common approach in the literature (e.g., in macroeconomic models of monopolistic competition), null-measure firms do not ignore the impacts of their decisions on aggregate outcomes. Firms pay at least some attention, believing that $\partial Y/\partial Y_i = q \in (0, 1]$. In this case, all the above equations, including (7) and (8), would hold *exactly* if (i) η is replaced by η/q and (ii) integrals are used instead of sums (e.g., $Y \equiv \int_0^N Y_i di$ and

$\mathrm{E}_a\left(h(A)\right) = \int_{\underline{A}}^{\overline{A}} h(A)\frac{g(A)}{1-G(\underline{A})}dA$, where g is now a density function).[3] These equations hold exactly because the profit of the least productive active firm is now precisely zero, due to the possibility of infinitesimal firm entries. Since the two models have essentially the same equations, they exhibit similar properties: (i) $\Omega \in (0, 1]$, (ii) Ω strictly increases with $\underline{A}$, and (iii) $\Omega \to 1$ as $\underline{A} \to \overline{A}$.

3 Quantification strategy

In this section, we outline the calibration strategy. Our primary empirical objective is to compute allocative efficiency Ω, which requires solely the distribution of firms' productivity (see Equation (5)). Thus, we aim to utilize real-world data to pin down the distributional parameters. We propose a two-stage procedure. In the first stage, we employ the calibration algorithm of Martinez and Santos (2024), finding, for a given distributional shape, $\underline{A}$ and $\overline{A}$ by matching aggregate TFP $\overline{A}\Omega$ and average markup μ. In the second stage, relying on this first-stage algorithm, we recover the distributional shape from the labor concentration measure $N_a HHI_L$. We detail this two-stage calibration procedure below. Before that, we discuss our distributional assumption and the computation of the target moments using real-world data.

3.1 Distributional assumption

Following Martinez and Santos (2024), we assume firm productivity is truncated Pareto distributed with shape parameter $k \neq 0$, consistent with the continuous version of their model. The calibration requires a mapping between the model's results and the productivity distribution. For the Pareto case, this is given by

$$\mathrm{E}_a\left((\underline{A}/A)^j\right) = \begin{cases} \left(\frac{k}{k+j}\right)\left(\frac{\tilde{A}^{k+j}-1}{\tilde{A}^{k+j}-\tilde{A}^j}\right) & \text{, if } k+j \neq 0 \\ \left(\frac{k\tilde{A}^k}{\tilde{A}^k-1}\right)\ln\tilde{A} & \text{, if } k+j = 0 \end{cases} \tag{9}$$

for $k \neq 0$, $j \in \mathbb{N} \setminus \{0\}$, and $\tilde{A} \equiv \overline{A}/\underline{A} > 1$, as shown in Martinez and Santos (2024).

3.2 Computing the target moments using real-world data

We consider three target moments: (i) the aggregate TFP $\overline{A}\Omega$, (ii) the cost-weighted average of firm-level markups μ, and (iii) the labor concentration measure $N_a HHI_L$. As discussed in Martinez and Santos (2024), the first two moments can be readily obtained using standard macroeconomic data and the parameter α. While TFP is backed out as a residual from the

[3] In the discrete model, $\eta > 1$ is sufficient for the second-order condition (SOC) for firms' profit maximization to hold. In the continuous case, $\eta > 0$ or $q \in (0, 1]$ should be low.

aggregate production function (4), using $\overline{A}\Omega = \frac{Y}{K^{\alpha}L^{1-\alpha}}$, the average markup is calculated as $\mu = \frac{1-\alpha}{LS}$, where LS denotes the labor share of national income.

However, obtaining a representative $N_a HHI_L$ for the entire economy proves challenging even with comprehensive firm-level data, as it involves the complex task of defining the relevant market for each firm in the economy (see Berry et al. 2019, Syverson 2019, and Benkard et al. 2021 for a discussion). This is why we pursue a weaker moment match for $N_a HHI_L$, trying only to approximate the shape of its time series by targeting the moment normalized. After all, in this case, we do not need to estimate $N_a HHI_L$ precisely as both its mean and variance are irrelevant, allowing us to rely on relatively aggregate employment data and simple assumptions regarding the relevant markets. The computation involves plugging estimates of firm-level employment data into $N_a HHI_L = N_a \sum_{i=1}^{N} (L_i/L)^2$, as discussed in detail in Section 4.4.

3.3 Two-stage calibration procedure

Given our distributional assumption and the computed data moments, we quantify the model using a two-stage procedure. In this process, we parsimoniously assume k is time-invariant.

First stage. For a given shape parameter $k \neq 0$, we compute $\underline{A}$ and $\overline{A}$ by matching aggregate TFP $\overline{A}\Omega$ and cost-weighted average markup μ, on a period-by-period basis. Martinez and Santos (2024) demonstrate that a unique solution for this calibration problem exists if and only if $\mu > 1$ and $k < 2/(\mu - 1)$. Under such conditions, given data on $\overline{A}\Omega$ and μ, the unique solution for $\underline{A}$ and $\overline{A}$ can be found using the following algorithm:

1. Given Equation (9), calculate $\tilde{A} \equiv \overline{A}/\underline{A}$ by numerically solving

$$\mu = \frac{1 - \mathrm{E}_a\left(\underline{A}/A\right)}{\mathrm{E}_a\left[(\underline{A}/A)(1 - \underline{A}/A)\right]}, \tag{10}$$

   which is derived from (5) and (6) holding exactly as in the continuous model.

2. From Equation (6) holding exactly, compute $\underline{A} = \overline{A}\Omega/\mu$.

3. Given $\tilde{A} \equiv \overline{A}/\underline{A}$ and $\underline{A}$ obtained from the previous steps, calculate $\overline{A} = \tilde{A} \times \underline{A}$.

From Equation (10), the average markup μ identifies $\tilde{A}$, which is a measure of technology dispersion, reflecting the productivity gap between the most and least productive active firms. As a consequence, for a given $k \neq 0$, allocative efficiency Ω is solely a function of μ, since computing Equation (5) requires only $\tilde{A}$ under (9). Figure 1 plots this function Ω of μ for truncated Pareto distributions with $k = 3, 5, 9$, and a uniform distribution ($k = -1$). Several points are noteworthy. First, Ω is strictly decreasing in $\mu = \frac{1-\alpha}{LS}$ and, thus, strictly increasing in LS. In particular, $\Omega \to 1^{-}$ as $\mu \to 1^{+}$. Intuitively, a lower average markup $\mu > 1$ indicates a less distorted economy, being associated with enhanced allocative efficiency Ω. Second, given a time series of μ, a lower k results in a higher and less volatile estimated Ω.

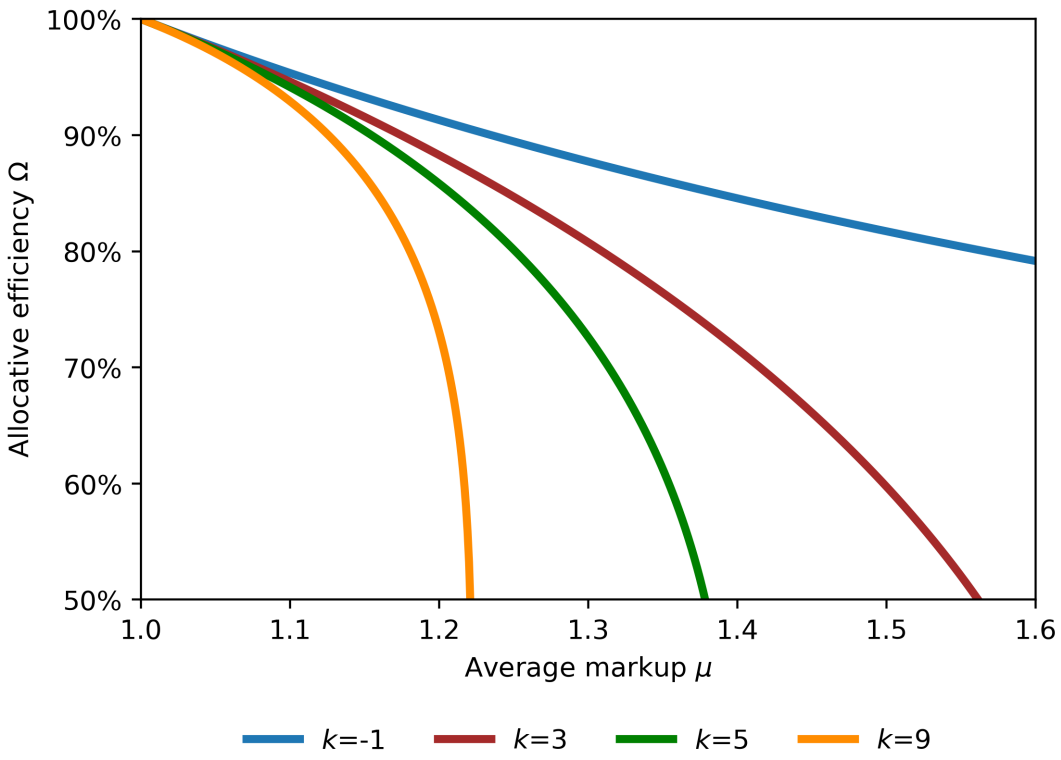

Figure 1: Allocative efficiency Ω *versus* average markup μ.

Second stage. Given time series of $\overline{A}\Omega > 0$ and $\mu > 1$, the first-stage algorithm allows for the computation of $\underline{A}$ and $\overline{A}$ for all periods under any $k < 2/(\max\{\mu\} - 1)$, $k \neq 0$, where $\max\{\mu\}$ denotes the maximum μ in its time series. With $\underline{A}$ and $\overline{A}$ determined, we can compute several variables in the model, including $N_a HHI_L$ from Equation (7). Under such conditions, we find the time-invariant $k \neq 0$ by searching for the one that minimizes the Euclidean distance between the time series of $N_a HHI_L$ in the model and in the data, with both series normalized to have zero mean and unit variance.[4] Naturally, the search is limited to $k < 2/(\max\{\mu\} - 1)$. By analogous reasoning to that previously used for Ω, computing $N_a HHI_L$ requires only data on the average markup μ (for a given $k \neq 0$). As a result, the estimation of k is also independent of TFP data, meaning TFP data are not used to estimate Ω, not even indirectly through k. TFP data are required just to pin down $\underline{A}$ and $\overline{A}$. Therefore, to decompose TFP, we first estimate Ω using data on $N_a HHI_L$ and $\mu = \frac{1-\alpha}{LS}$, and then compute $\overline{A}$ from the actual TFP $\overline{A}\Omega$. Consequently, our two-stage procedure does not contradict the reasoning presented in Martinez and Santos (2024) regarding the residual from the production function. Specifically, in this model, the residual is not the TFP $\overline{A}\Omega$ itself, but rather only its technology component $\overline{A}$, which is cleaner as it excludes the effects of misallocation.

[4]This is equivalent to minimizing the sum of squared residuals of the normalized $N_a HHI_L$.

4 Data and parameters

This section describes the data and parameters used in our empirical exercise for Brazil. We begin in Section 4.1 by presenting the basic macroeconomic data, which are used to measure the key variables of our model, such as output Y and labor income share LS. In this initial part, we also discuss how varying input utilization is accounted for, involving an econometric estimation conducted in Section 4.3. This estimation relies on the production function, with the parameter α calibrated first in Section 4.2 using cost share data. Finally, Section 4.4 details the data and procedures used to compute the labor market concentration measure $N_a HHI_L$.

4.1 Basic data

We use an annual database, in which Y is the real GDP in 2010 prices, LS is the labor share of national income, and $\tilde{L}$ is the number of persons engaged, all sourced from the Table of Resources and Uses of National Accounts produced by the Brazilian Institute of Geography and Statistics (IBGE). The labor income share LS is calculated as the ratio of wages and social contributions to the sum of wages, social contributions, and gross operating surplus. As a consequence, self-employment income (mixed income) is allocated to labor and non-labor in the same proportions as the rest of the economy, following the preferred method of the Penn World Table 10.01 (Feenstra et al. 2015). In Section 6.3, we assess the impact of using alternative labor income share measures. Average annual hours worked by persons engaged, h, are also sourced from the Penn World Table 10.01, while capital stock in 2010 prices, $\tilde{K}$, is obtained from Souza Júnior and Cornelio (2020).

To calculate K and L, we adjust $\tilde{K}$ and $h\tilde{L}$ using the capacity utilization rate for manufacturing, γ, from the Getulio Vargas Foundation (FGV). This adjustment is implemented using a flexible approach, considering the following empirical version of the production function (4) for the year t:

$$Y_t = \overline{A}_t \Omega_t \tilde{K}_t^{\alpha} (h_t \tilde{L}_t)^{1-\alpha} \gamma_t^{\beta}. \tag{11}$$

The underlying assumption is that capital and labor utilization is simply a rescaling of an observable measure of input usage intensity, in line with Basu et al. (2006) and Basu et al. (2013). As Basu et al. (2013, p.43) argue, "a cost-minimizing firm operates on all margins simultaneously, both observed and unobserved. As a result, changes in observed margins can proxy for unobserved utilization changes." Basu et al. (2006) derive this result from a dynamic cost-optimizing problem in which the firm, subject to adjustment costs, seeks to minimize the present discounted value of its costs. While they use hours worked as a proxy for input usage, we rely on a capacity utilization survey, following Comin et al. (2023).

Equation (11) contains two unknown parameters, α and β. While both could, in principle, be estimated econometrically, we find that (i) the estimates are highly sensitive to the specific

empirical strategy and estimator used, and (ii) α tend to be either implausibly high or, if no capacity utilization adjustment is made (i.e., β is set to 0), implausibly low. As a result, we opt to first calibrate the capital share parameter α and only then pursue an econometric estimation of β. This sequential approach mirrors the methodology of Basu et al. (2006) and Basu et al. (2013).

4.2 Calibration of the Cobb-Douglas capital share parameter

Since firms use inputs optimally, it follows that α is equal to the cost share of capital, i.e., $\alpha = \frac{Kr}{Kr+Lw}$. Thus, we can calibrate α using cost share data, as Martinez and Santos (2024) do for the US. Labor expenses Lw are readily available from National Accounts. The main challenge lies in accurately calculating capital expenses, distinguishing them from pure profit. To address this, we follow Barkai (2020) and compute a required rate of return in the spirit of Hall and Jorgenson (1967). Capital expenses are then obtained by multiplying this rate by the nominal value of the capital stock. We perform this calculation for each type of capital listed in Souza Júnior and Cornelio (2020): (i) residential structures, (ii) infrastructure, (iii) other structures, (iv) machinery and equipment, and (v) others.

Ignoring any tax treatment, the required rate of return for capital type s is calculated as the nominal weighted average cost of capital (WACC) minus the expected inflation for capital s, plus the depreciation rate of capital s. Depreciation rates are sourced from Souza Júnior and Cornelio (2020), while expected inflations are assumed to be equal to realized inflations, as computed using the Table of Resources and Uses of National Accounts. The WACC is taken from Santos (2020), where Brazilian firms are supposed to finance investment solely through (i) equity or (ii) debt with the Brazilian Development Bank (BNDES). The debt weight is given by the share of BNDES lending for capital goods in private sector gross capital formation. The debt interest rate is the BNDES lending rate for capital goods, while the equity rate is the Pre-DI swap 360 days plus the Equity Risk Premium (ERP) calculated by Carvalho and Santos (2020).[5]

These data enable us to calculate the share of capital expenses in total expenses from 2002 to 2017, as shown in Figure 2. Using this time series, we estimate an autoregressive process of order one and use its steady state to calibrate α. The rationale behind this procedure is that the assumption of optimal use of inputs is a better approximation in the long run, as actual input usage can deviate significantly from optimal static levels in the short run, particularly for capital. We find $\alpha = 0.39$, higher than the standard calibration $\alpha = 1/3$. This result is robust to several variations in the calculation of the required rate of return. First, computing the equity rate using the Pre-DI swap 1800 days still yields $\alpha = 0.39$. Second, using expected 12-month consumer inflation from the Focus survey instead of realized capital inflations does not alter the estimate either. Third, assigning zero weight to debt, thereby making the WACC equal to the

[5]"The Pre-DI swap contract traded at the BM&FBovespa, the Brazilian Stock Exchange, is an interest rate swap where one of the parties agrees to make pre-fixed interest payments in exchange for receiving floating interest payments based on the DI rate, whereas the other assumes a reverse position" (Carvalho and Santos 2020, p.12).

equity rate, only slightly increases the estimate to $\alpha = 0.40$. Finally, we incorporate corporate income tax following Barkai (2020), using a 34% corporate (IRPJ/CSLL) tax rate. We consider two scenarios for the capital cost recovery rate, which is the net present value of depreciation allowances for capital. Firstly, a recovery rate of 100% results in $\alpha = 0.38$. Secondly, reducing the recovery rate to 70.71%, the OECD average level in 2021 according to the Tax Foundation, increases the estimate, but not by much, to $\alpha = 0.41$.

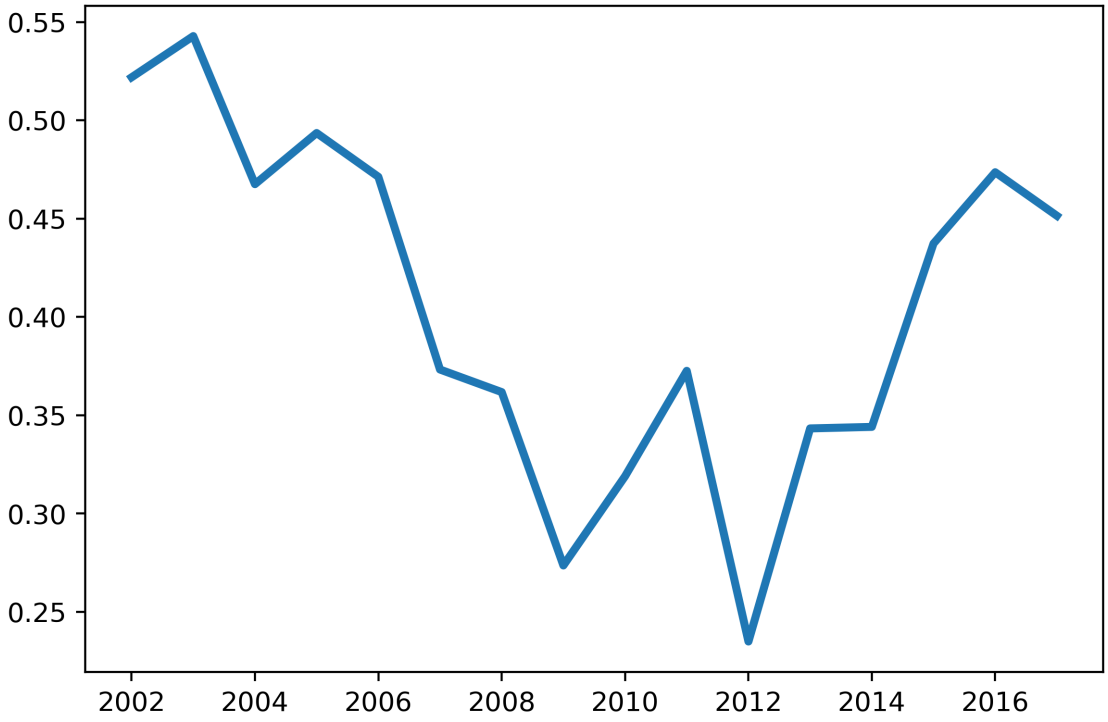

Figure 2: Capital expenses as a share of total capital and labor expenses.

4.3 Estimation of the adjustment for input utilization

Let $\Delta \ln(\overline{A}_t \Omega_t) = c + \xi_t$, where Δ represents the first difference operator, $\mathrm{E}(\xi_t | I_{t-1}) = 0$, and I_{t-1} denotes the information set at time $t-1$. Hence, from Equation (11),

$$\Delta \ln Y_t = c + \alpha \Delta \ln \tilde{K}_t + (1-\alpha)\Delta \ln(h_t \tilde{L}_t) + \beta \Delta \ln \gamma_t + \xi_t. \tag{12}$$

We set $\alpha = 0.39$ and estimate c and β using Equation (12), exploring the moment conditions $\mathrm{E}\left(X_{t-1} \cdot \xi_t\right) = 0$, where X_{t-1} is a vector of instrumental variables such as $X_{t-1} \in I_{t-1}$. This estimation methodology is grounded in the dynamic panel literature on production function estimation (e.g., Blundell and Bond 2000), particularly the simplified model presented in Ackerberg et al. (2015). However, we apply it to time series rather than panel data. Alternatively, we could have used the method of Olley and Pakes (1996) or its extensions Levinsohn and Petrin (2003) and Ackerberg et al. (2015). Nevertheless, given $\Delta \ln(\overline{A}_t \Omega_t) = c + \xi_t$, these methods

are equivalent to our own if all productivity shocks in (12) affect input decisions, as their first stage can be ignored in this case. This assumption seems plausible here since input utilization rates can be quickly adjusted. Empirical evidence also supports this, as we find no evidence of serial correlation in the error term.[6] Additionally, these alternative methods require estimating a sufficiently flexible nonparametric function in their first stage (e.g., high-order polynomial), which poses challenges due to our limited sample size (with no more than 24 observations).

Our instruments, X, include a constant, $\ln \tilde{K}_t$, $\ln \tilde{K}_{t-1}$, $\ln(h_{t-1}\tilde{L}_{t-1})$, $\ln(h_{t-2}\tilde{L}_{t-2})$, $\ln \gamma_{t-1}$, $\ln \gamma_{t-2}$, $\ln Y_{t-1}$, and $\ln Y_{t-2}$. Assuming all productivity shocks influence input decisions, these are the instruments recommended by Ackerberg et al. (2015), with an additional lag of each variable to better accommodate the first differences in (12). We apply the Two-Stage Least Squares (2SLS) estimator for this analysis. For completeness, we also estimate (12) using Ordinary Least Squares (OLS).

Table 1 presents the estimates derived from annual data between 1998 and 2019.[7,8] The results reject both the no-adjustment case ($\beta = 0$) and the common practice of applying γ only to capital ($\beta = \alpha = 0.39$), as the β estimates are considerably higher than $\alpha = 0.39$. The impact of a higher β on estimated TFP is shown in Figure 3, which compares TFPs under (i) no adjustment ($\beta = 0$), (ii) standard adjustment ($\beta = \alpha = 0.39$), (iii) OLS estimate ($\beta = 0.66$), and (iv) 2SLS estimate ($\beta = 0.74$). As the figure illustrates, a higher β produces a smoother TFP, particularly around the economic crises of 2008 and 2015–2016. As discussed in Section 3.3, estimating allocative efficiency Ω does not require TFP data, meaning a smoother TFP results in a smoother technology frontier $\overline{A}$, with no effect on Ω.

Table 1: Estimates of the parameters in the production function (12) for $\alpha = 0.39$

Parameter	OLS	2SLS
c	0.01***	0.01***
	(0.002)	(0.003)
β	0.656***	0.744***
	(0.089)	(0.095)

Parenthesis: Heteroskedasticity-robust standard error.
Significance: * (10%), ** (5%), *** (1%).
Sample (adjusted): 1998–2019 (22 observations).

In what follows, we use the 2SLS β estimate, as it is consistent under the assumptions considered here. In any case, this choice is not crucial for our empirical results, since the TFPs computed using 2SLS and OLS β estimates are very similar, as shown in Figure 3.

[6] If $\ln(\overline{A}_t\Omega_t) = \omega_t + \epsilon_t$, where $\Delta\omega_t = c + \xi_t$ and ϵ_t denotes white-noise productivity shocks not considered in input decisions, the error term in (12) would be $\xi_t + \Delta\epsilon_t \sim MA(1)$. A similar result applies under the more general assumption $\omega_t = c + \rho\omega_{t-1} + \xi_t$, when "$\rho$-differentiating" (11) gives an expression analogous to (12), with error term $\xi_t + (\epsilon_t - \rho\epsilon_{t-1}) \sim MA(1)$ (Blundell and Bond 2000).

[7] The dataset spans from 1996 to 2019, but we lose the first two observations due to the use of lagged variables.

[8] We also tested two Generalized Methods of Moments (GMM) estimators from Hansen (2020) that are asymptotically efficient under heteroskedasticity: (i) two-step GMM, using 2SLS in the first step, and (ii) iterated GMM. The β estimates are only slightly higher (0.838 and 0.846, respectively), resulting in nearly equivalent TFPs.

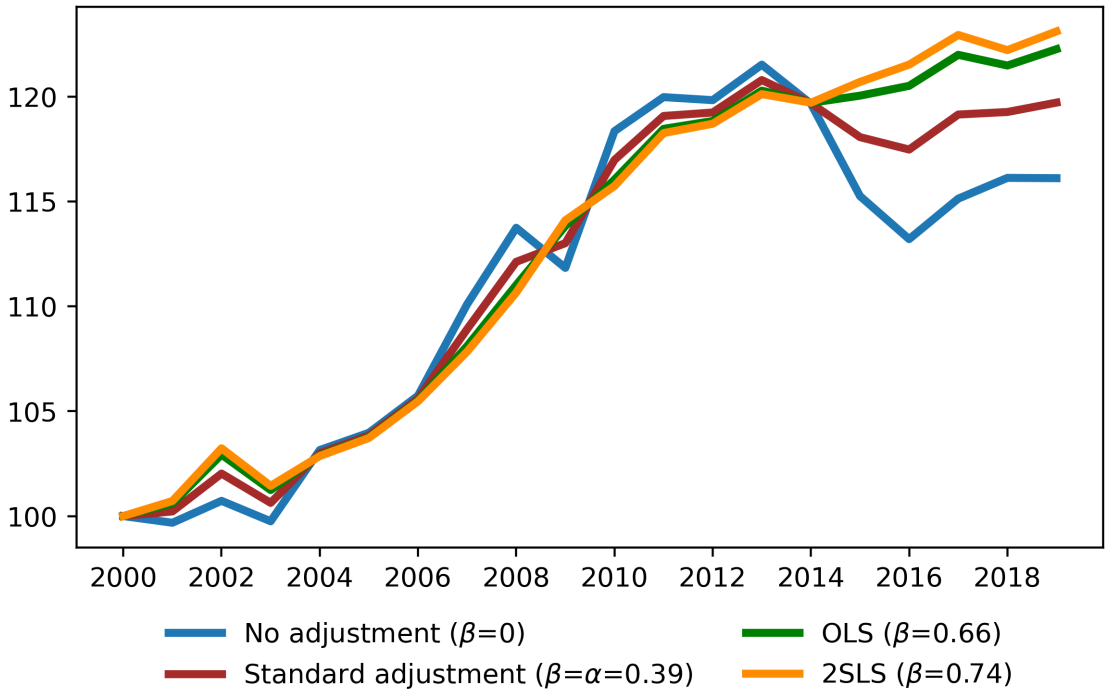

Figure 3: TFP under various β values (2000=100).

4.4 Labor market data

We estimate $N_a HHI_L$ without using firm-level data, relying instead on two tables from the Central Register of Enterprises (CEMPRE), provided by IBGE. The first table presents the total number of firms, total employment, and the number of firms and employment categorized into nine size bins based on the number of employees.[9] The second table reports the total number of firms, total employment, and the employment share of the 4, 8, and 12 largest firms (by number of employees). Although CEMPRE covers all formal organizations, this second table is limited to formal corporate entities. As a consequence, we opt not to include data from other formal organizations, namely public administration and non-profit organizations, in the first table either. This focus on corporate entities ensures comparability between the tables and also aligns with the model utilized in this paper, where firms are profit-maximizing.

These two tables are available from 2006 to 2020 for all sectors (up to the 3-digit level) from the National Classification of Economic Activities (CNAE) 2.0, a Brazilian classification derived from ISIC Rev.4. Using these data, we follow five steps to compute $N_a HHI_L$.

Step 1 – addressing missing data. The IBGE omits some employment information to prevent the identification of individual firms. To address this, for each 2-digit and 3-digit sector and year, we perform three imputations:

1. Use the total employment from one table to fill in missing values in the other.

[9]The size bins are 0 to 4, 5 to 9, 10 to 19, 20 to 29, 30 to 49, 50 to 99, 100 to 249, 250 to 499, and 500 or more.

2. Estimate missing employment data for a given firm size bin by calculating the simple average of the bin's bounds and multiplying it by the respective number of firms.[10,11]

3. If no further data is missing, we multiply all imputed employment in the size bins by a scalar, ensuring the sum of employment in the bins matches the total employment figure. If only one piece of data remains missing, it is backed out as a residual. If more than one value is still missing, the data for that sector and year are discarded.

Naturally, the second imputation is not applied to the last bin (500 or more employees), as its upper bound is unknown. For the first bin (0 to 4 employees), while the imputation can be applied, the results may be distorted due to firms with no employees (e.g., if the number of such firms is disproportionately high). Therefore, we consider two approaches for the first bin: either applying or omitting the second imputation procedure.

Step 2 – estimating employment per firm. Let $b = \{500, 250, 100, ..., 0\}$ be the set of lower bounds of firms' size bins from the first table, b_k be the k-th largest element of b, and N_j be the number of firms with j or more employees. Thus, using the two tables (with missing data addressed in Step 1), we determine, for each available 2-digit and 3-digit sector and year, the total employment of the i largest formal enterprises, for $i \in I = \{4, 8, 12, N_{b_1}, N_{b_2}, ..., N_{b_9}\}$. We then use this information to estimate firm-level employment. Denoting the j-th smallest element of I by i_j for $j \in \{1, 2, ..., 12\}$, with $i_0 = 0$, we estimate employment per firm by supposing firms ranked $(i_{j-1} + 1)$ to i_j have the same size. This approach ensures the estimated firm sizes fall within the bounds specified in the first table.

Since the first bin (0 to 4 employees) includes firms with no employees, we also consider two alternative approaches to adjust the data before applying the procedure just described. First, we exclude all data from the first bin, thus considering only $j \in \{1, 2, ..., 11\}$. Second, we retain $j \in 1, 2, ..., 12$ but replace $N_{b_9} = N_0$ by N_1, effectively excluding firms with no employees from the first bin. As the IBGE does not disclose the number of such firms, we estimate it by assuming firms with 1 to 4 employees have, on average, $\frac{1+4}{2} = 2.5$ employees. Hence, the new number of firms in the first bin is computed by dividing its total employment by 2.5.

Step 3 – computing the results for each sector and year. Using the employment per firm estimated in Step 2, we calculate, for each available 2-digit and 3-digit sector and year, the number of active firms N_a and the labor market concentration index $HHI_L \equiv \sum_{i=1}^{N} (L_i/L)^2$.

Step 4 – selecting the sectors. We now select the sectors to be used in computing aggregate results, ensuring they are representative of the entire economy and suitable for model calibration. We consider two alternative sets of sectors. First, we use all 3-digit sectors, as they are

[10] This assumes the average number of employees per firm in a given bin equals the simple average of the bin's employment bounds.

[11] For example, if a sector in a given year has 10 firms with 5 to 9 employees, employment is estimated as $\frac{5+9}{2} \times 10 = 70$.

comprehensive, define the narrowest possible markets in the data, and rely on the most granular information available to estimate employment per firm, which enhances precision.[12] Second, we select only the 3-digit sectors that do not belong to a 2-digit sector with a high share of non-enterprise formal organizations or that are considered unsuitable for the model of Martinez and Santos (2024) (e.g., utilities).[13]

These initial sets of sectors are then adjusted to ensure the sectoral coverage remains constant over time, avoiding distortions caused by changes in the sectors included each year. We use two different methods. First, if a selected 3-digit sector is missing in Step 3 for at least one year, we exclude all 3-digit sectors within the corresponding 2-digit sector and, if data are available for all years, include this 2-digit sector. Second, we simply exclude all selected 3-digit sectors with missing data in Step 3.

Step 5 – aggregating the results. Using the results from Step 3 for all sectors selected in Step 4, we employ three methods to obtain the aggregate results for each year. First, assuming a single national market, we compute N_a as the total number of firms across all selected sectors, and HHI_L by plugging the employment of each firm in the selected sectors directly into $HHI_L = \sum_{i=1}^{N} \left(\frac{L_i}{L}\right)^2$. Second, we compute $N_a HHI_L$ for each selected sector and take the average. Third, we calculate $N_a HHI_L$ for each selected sector and use the median value.

Table 2 summarizes all the methods applied in computing the aggregate results, as discussed in the presentation of the five steps. We use all possible combinations of these methods, resulting in $2 \times 3 \times 2 \times 2 \times 3 = 72$ different time series of $N_a HHI_L$.

5 Results

Using the method discussed in Section 3 and the data and parameters from Section 4, we obtain k, $\underline{A}$, and $\overline{A}$ for Brazil in two steps. First, for a given time series of $N_a HHI_L$, we estimate the model from 2006 to 2019, finding the time-invariant k. Second, with this k set, we estimate all other model parameters from 2000 to 2019 using the first-stage algorithm of the quantification method. Figure 4 presents the results based on $N_a HHI_L$ as determined by the baseline methods

[12] In this estimation, we suppose some firms are of the same size, which is a strong assumption. However, this assumption becomes weaker with more granular data, since the number of firms assumed to have exactly the same size decreases.

[13] The 19 excluded 2-digit sectors are: 35 – Electricity, gas and other utilities, 36 – Water collection, treatment and distribution, 37 – Sewage and related activities, 38 – Collection, treatment and disposal of waste, and material recovery, 39 – Decontamination and other waste management services, 68 – Real estate activities, 72 – Scientific research and development, 81 – Services for buildings and landscape activities, 84 – Public administration, defense and social security, 85 – Education, 86 – Human health care activities, 87 – Human health care activities integrated with social assistance, provided in collective and private residences, 88 – Social assistance services without accommodation, 90 – Artistic, creative and entertainment activities, 91 – Activities related to cultural and environmental heritage, 92 – Gambling and betting exploration activities, 93 – Sports, recreation and leisure activities, 94 – Activities of associative organizations, and 99 – International organizations and other extraterritorial institutions.

Table 2: Alternative methods to compute $N_a HHI_L$

Step	Topic	Method
1	Imputation in the first bin (0 to 4 employees)	(i) Average bin bounds $\times$ number of firms (ii) Backed out as a residual (if possible)*
2	Data from the first bin (0 to 4 employees)	(i) Included (ii) Included only for firms with employees* (iii) Excluded
4	Initial set of sectors	(i) All 3-digit sectors* (ii) Only selected 3-digit sectors
4	Sectors with missing data	(i) Replaced by the corresponding 2-digit sectors* (ii) Excluded
5	Aggregation method	(i) National market (ii) Sectors' average (iii) Sectors' median*

*Baseline methods.

outlined in Table 2, which yield $k = 3.19$. Choosing any of the 72 time series of $N_a HHI_L$ would yield similar results, though, as all estimates of k are very close, ranging between 3 and 3.3. Note the results shown in Figures 4a, 4b, 4c, and 4d do not depend on TFP data. Therefore, they are robust to different measures of labor and capital, including variations due to alternative adjustments for input utilization. Only Figure 4e relies on TFP data, making it sensitive to input measurements.

Consistent with our quantification strategy, the model perfectly reproduces TFP $\overline{A}\Omega$ and the average markup μ, but not $N_a HHI_L$, as we aim only to minimize the distance to this moment normalized. This is shown in Figure 4a, where the actual $N_a HHI_L$ is normalized to match the average and standard deviation of the model's time series from 2006 to 2019. In any case, the model fits the normalized data well, with a correlation of 0.67 and capturing the observed upward trend. It is also worth noting the model series varies very little, remaining between 1.332 and 1.335.

Another way to assess the model fit is by evaluating the number of active firms N_a. To compute the actual number of firms, we use data from Section 4.4 and the baseline methods highlighted in Table 2, but now applied to N_a.[14] To compute N_a in the model, we use Equation (3), with η replaced by η/q as in its continuous version, assuming η/q is time-invariant. Analogous to $N_a HHI_L$, accurately identifying the level of the actual N_a requires knowing the relevant market for each firm in the economy. Given this, we evaluate the model fit only after a normalization, as shown in Figure 4b, where both series are divided by their 2006–2019 averages. This approach allows us to choose any feasible adjusted elasticity η/q (e.g., $\eta/q = 1$), since changing it would simply multiply the model series by a constant. As can be seen, even though it is not a target moment, the model has a good fit, with the series being highly corre-

[14]Hence, for each year, we calculate N_a for all selected sectors and then take the median to obtain the representative value.

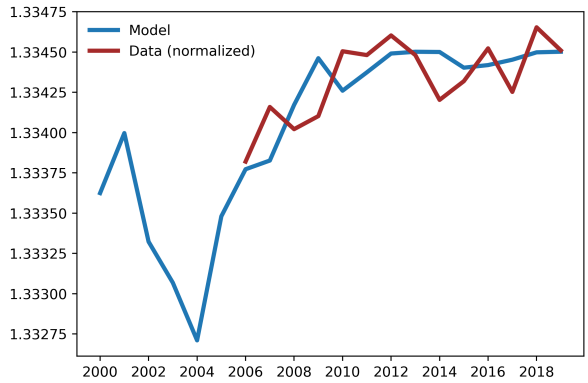

(a) Labor market concentration measure $N_a HHI_L$

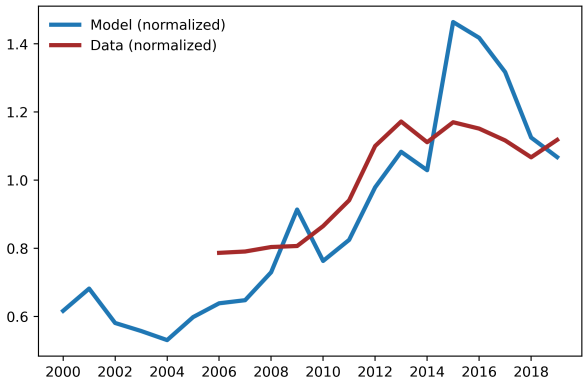

(b) Number of active firms N_a

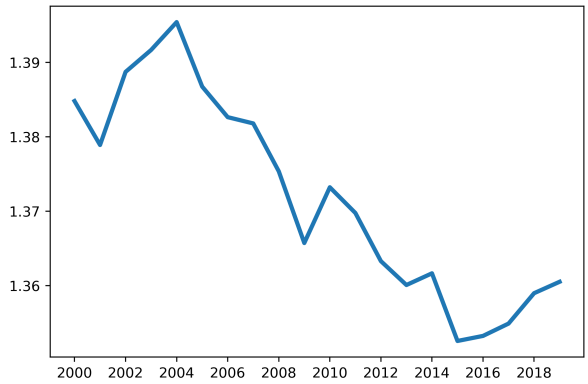

(c) Product market concentration measure $N_a HHI_s$

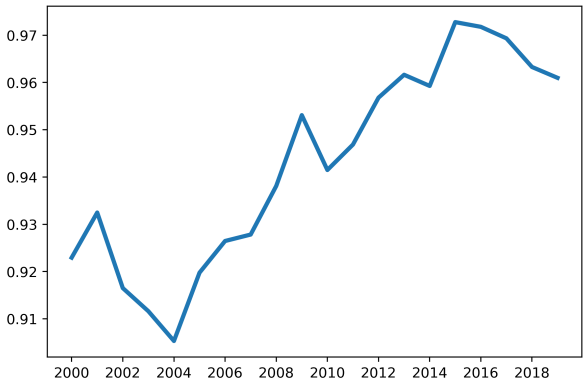

(d) Allocative efficiency Ω

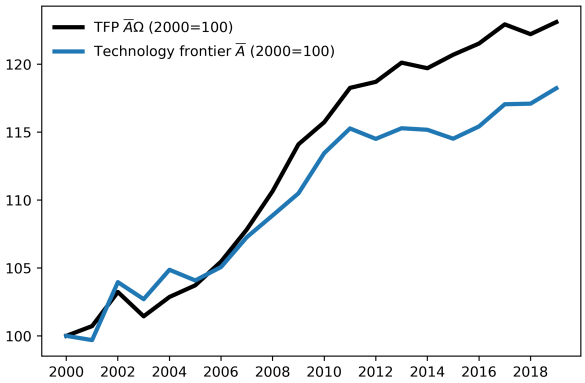

(e) TFP $\overline{A}\Omega$ and technology frontier $\overline{A}$

Figure 4: Estimates for the baseline model.

lated (correlation of 0.85) and the model capturing the observed upward trend. The errors are concentrated around periods of economic crises (2008–2009 and 2015–2016), when the static model of Martinez and Santos (2024) is expected to perform poorly.[15] For instance, during these times, firms' use of labor input is probably far from optimal, meaning $\frac{1-\alpha}{LS}$ would not properly measure the cost-weighted average of markup μ.

We could assess the concentration in the product market using $N_a HHI_s$. Unfortunately, we do not have the information required to compute it using actual data, but we can obtain the model's predictions from Equation (8). Figure 4c displays these estimates, which indicate an increase in product market concentration until 2004, a downward trend between 2005 and 2015, and a slight increase from 2016 to 2019. Additionally, $N_a HHI_s$ and $N_a HHI_L$ behave very differently: they are negatively correlated (correlation of -0.92), and $N_a HHI_s$ exhibits much more variation.

Figure 4d presents the estimated allocative efficiency Ω. It shows an upward trend, reflecting the observed increase in the labor income share and, consequently, the estimated decrease in the average markup. This is a sharp contrast with most developed countries, which have experienced a decreasing labor share and increasing average markup over the last decades (e.g., Calligaris et al. 2018, De Loecker and Eeckhout 2018, and Autor et al. 2020). Accordingly, Baqaee and Farhi (2020) find the distance from optimal allocation widened in 2015 compared to 1997 in the US. Moreover, note Ω exhibits trends similar to $N_a HHI_s$, but with reversed signs (correlation of -0.9998): it decreases until 2004, increases from 2005 to 2015, and slightly decreases from 2016 onwards. Thus, $N_a HHI_s$ appears to be a good proxy for Ω, with higher (lower) $N_a HHI_s$ indicating lower (higher) Ω. Finally, Ω is procyclical, showing a correlation of 0.88 with GDP.

Therefore, allocative efficiency Ω increases during booms and decreases during busts, similar to TFP $\overline{A}\Omega$, which exhibits a 0.97 correlation with GDP. This suggests that TFP net of allocative efficiency effects, represented by the technology frontier $\overline{A}$, should exhibit more stable growth compared to TFP. This is illustrated in Figure 4e, which plots $\overline{A}\Omega$ and $\overline{A}$, both adjusted to equal 100 in 2000. Using these adjusted series, we find a standard deviation of 8.39 for $\overline{A}\Omega$ and 6.01 for $\overline{A}$. Similarly, when detrending both series using linear trends, TFP shows a higher standard deviation (1.93) compared to $\overline{A}$ (1.54). These results are easier to see in Table 3, which presents the average annual growth of GDP Y, TFP $\overline{A}\Omega$, technology frontier $\overline{A}$, and allocative efficiency Ω for the full sample (2000–2019) and four subperiods: (i) the pre-boom period (2000–2003), (ii) the boom period (2003–2007), (iii) the crises period (2007–2016), and (iv) the post-crises period (2016–2019). The results for these subperiods show TFP $\overline{A}\Omega$ is more volatile than the technology frontier $\overline{A}$, which exhibits a relatively stable growth rate: 0.89% for 2000–2003, 1.09% for 2003–2007, 0.82% for 2007–2016, and 0.81% for 2016–2019.

These results suggest TFP cycles are primarily driven by changes in allocative efficiency.

[15] Brazil experienced an intense economic crisis during 2015–2016, with GDP falling 7% in 2015 and 2016 (3.4% per year).

Table 3: Average annual growth of GDP, TFP, and its components for the baseline model, %

Variable	2000–19	Subperiods			
		2000–03	2003–07	2007–16	2016–19
GDP Y	2.28	1.86	4.74	1.62	1.44
TFP $\overline{A}\Omega$	1.1	0.48	1.54	1.34	0.43
Technology frontier $\overline{A}$	0.89	0.89	1.09	0.82	0.81
Allocative efficiency Ω	0.21	-0.41	0.44	0.52	-0.37

For instance, the rapid productivity gains observed between 2003 and 2016 are largely attributable to Ω, which grows at 0.5% per year during this period, compared to -0.4% in 2000–2003 and 2016–2019. In contrast, the technology frontier grows more steadily, indicating $\overline{A}$ is the most structural component of TFP. This annual technology growth rate of 0.9% can be interpreted as the current long-run growth level of Brazilian TFP, since $\Omega \in (0, 1]$ and consequently it cannot increase or decrease indefinitely.

6 Robustness

In this section, we conduct four robustness exercises. First, we consider a uniform distribution by setting $k = -1$, when the model quantification requires *only* macroeconomic data. As argued in Martinez and Santos (2024), given the reasonable and common assumption that high-productivity firms are relatively scarce, this value of k yields the most conservative results compared to standard growth-accounting exercises, which attribute all TFP variations to technology changes. Second, instead of our baseline calibration of $\alpha = 0.39$, we explore the standard $\alpha = 1/3$ and $\alpha = 0.41$, the highest calibration from Section 4.2. Third, we experiment with alternative labor income share series, treating self-employment income (mixed income) differently. Finally, we select a distribution for firm market share that is consistent with Zipf's law, rather than imposing a productivity density as done in Section 3.1. Overall, these exercises do not disprove the main conclusions presented in Section 5.

6.1 Shape parameter of the truncated Pareto distribution

As discussed in Section 3.3 based on Figure 1, changes in LS appear to have a smaller impact on Ω when k is lower. This suggests reducing k would result in a less volatile allocative efficiency Ω and, consequently, a more volatile technology frontier $\overline{A}$. In other words, a lower k would yield more conservative results compared to standard growth-accounting exercises, where all TFP growth is attributed to technology improvement. Indeed, Martinez and Santos (2024) show $\Omega \to 1$ as $k \to -\infty$, causing their model's residual $\overline{A}\Omega$ to converge to the standard growth-accounting residual $\overline{A}$ in this limiting case. Consequently, it would be useful to establish a lower bound for k. As argued by Martinez and Santos (2024), assuming high-productivity

firms are relatively scarce, this lower bound is $k = -1$, since the truncated Pareto density is downward sloping only for $k > -1$, $k \neq 0$, becoming upward sloping for $k < -1$ and constant for $k = -1$ (uniform distribution). This assumption is not only economically reasonable but is also commonly adopted, often by imposing a non-truncated Pareto distribution for firms' productivity. In short, the most conservative reasonable TFP decomposition is achieved when productivity is uniformly distributed.

Table 4 presents the new TFP decomposition, computed using the first-stage algorithm of the quantification method, which relies solely on macroeconomic data. In this approach, $\mu = \frac{1-\alpha}{LS}$ is used to estimate Ω, with $\overline{A}$ subsequently backed out as a residual from the TFP $\overline{A}\Omega$. The results reveal expected differences, particularly the higher variability in the growth of $\overline{A}$ across the subperiods under $k = -1$. However, the technology component $\overline{A}$ continues to grow more steadily than the TFP $\overline{A}\Omega$, with TFP cycles typically driven by allocative efficiency Ω. All in all, the main findings appear robust to conservatively setting $k = -1$.

6.2 Share parameter of the Cobb-Douglas production function

In Section 4.2, we calibrated $\alpha = 0.39$ using cost share data. Here, we assess the robustness of our results to this parameter choice. Specifically, we re-estimate the model parameters (including β) for (i) the lower standard $\alpha = 1/3$ and (ii) $\alpha = 0.41$, the highest calibration from Section 4.2, obtained by adding corporate income tax and adjusting the capital cost recovery rate to the 2021 OECD average level. As shown in Table 4, the results for $\alpha = 0.41$ are practically identical to the baseline findings. More noticeable differences emerge with $\alpha = 1/3$, but the main conclusions remain valid: the technology frontier $\overline{A}$ grows more steadily than TFP $\overline{A}\Omega$, and TFP cycles are driven by allocative efficiency Ω. A noteworthy difference is that $\overline{A}$ decelerated during the TFP boom of 2003–2016, which is counterintuitive and suggests this value of α may be excessively low for Brazil.

6.3 Labor share of national income

One major challenge in computing the labor income share is accurately gauging the labor income of self-employed workers, as National Accounts typically only disclose the total income earned by such workers, known as mixed income. This is particularly important in developing countries like Brazil, where a substantial portion of the workforce is self-employed.[16] Gollin (2002) suggests various methods to address this challenge. One approach is to allocate mixed income to labor and non-labor in the same proportions as the rest of the economy. As discussed in Section 4.1, this method is our baseline methodology and is also the preferred method of the Penn World Table 10.01. Alternatively, Gollin (2002) proposes allocating all mixed income to labor, which provides an upper bound for the labor income share LS. A lower bound for LS

[16] In Brazil, approximately a quarter of employed individuals are self-employed, according to the 2012–2022 quarterly data from the National Household Sample Survey (PNAD), which is conducted by IBGE.

Table 4: Average annual growth of GDP, TFP, and its components, %

Variable	2000–19	Subperiods			
		2000–03	2003–07	2007–16	2016–19
Baseline model					
TFP $\overline{A}\Omega$	1.1	0.48	1.54	1.34	0.43
Technology frontier $\overline{A}$	0.89	0.89	1.09	0.82	0.81
Allocative efficiency Ω	0.21	-0.41	0.44	0.52	-0.37
Robustness #1: uniform distribution ($k = -1$)					
TFP $\overline{A}\Omega$	1.1	0.48	1.54	1.34	0.43
Technology frontier $\overline{A}$	0.95	0.74	1.26	0.95	0.74
Allocative efficiency Ω	0.15	-0.26	0.28	0.38	-0.3
Robustness #2: $\alpha = 1/3$					
TFP $\overline{A}\Omega$	1.13	0.49	1.52	1.43	0.36
Technology frontier $\overline{A}$	0.81	1.14	0.82	0.66	0.9
Allocative efficiency Ω	0.32	-0.64	0.69	0.76	-0.53
Robustness #3: $\alpha = 0.41$					
TFP $\overline{A}\Omega$	1.09	0.47	1.55	1.3	0.46
Technology frontier $\overline{A}$	0.9	0.83	1.17	0.85	0.79
Allocative efficiency Ω	0.18	-0.35	0.37	0.44	-0.32
Robustness #4: upper-bound LS series					
TFP $\overline{A}\Omega$	1.11	0.48	1.53	1.37	0.41
Technology frontier $\overline{A}$	1.07	0.79	1.55	1.09	0.68
Allocative efficiency Ω	0.03	-0.3	-0.02	0.27	-0.27
Robustness #5: lower-bound LS series					
TFP $\overline{A}\Omega$	1.09	0.47	1.55	1.29	0.46
Technology frontier $\overline{A}$	0.47	0.92	-0.02	0.39	0.94
Allocative efficiency Ω	0.61	-0.44	1.57	0.9	-0.47
Robustness #6: Zipf's law calibration ($k = 0.5$)					
TFP $\overline{A}\Omega$	1.1	0.48	1.54	1.34	0.43
Technology frontier $\overline{A}$	0.89	0.87	1.12	0.82	0.81
Allocative efficiency Ω	0.21	-0.39	0.42	0.51	-0.37
Robustness #7: Zipf's law calibration ($k = 1$)					
TFP $\overline{A}\Omega$	1.1	0.48	1.54	1.34	0.43
Technology frontier $\overline{A}$	0.89	0.87	1.11	0.82	0.81
Allocative efficiency Ω	0.21	-0.39	0.42	0.51	-0.37
Robustness #8: Zipf's law calibration ($k = 1.5$)					
TFP $\overline{A}\Omega$	1.1	0.48	1.54	1.34	0.43
Technology frontier $\overline{A}$	0.89	0.88	1.11	0.82	0.81
Allocative efficiency Ω	0.21	-0.39	0.42	0.51	-0.37

can be obtained by allocating no mixed income to labor, which is the naïve approach criticized by Gollin (2002). These three LS series are illustrated in Figure 5. While they are highly correlated, they exhibit different levels, as expected.

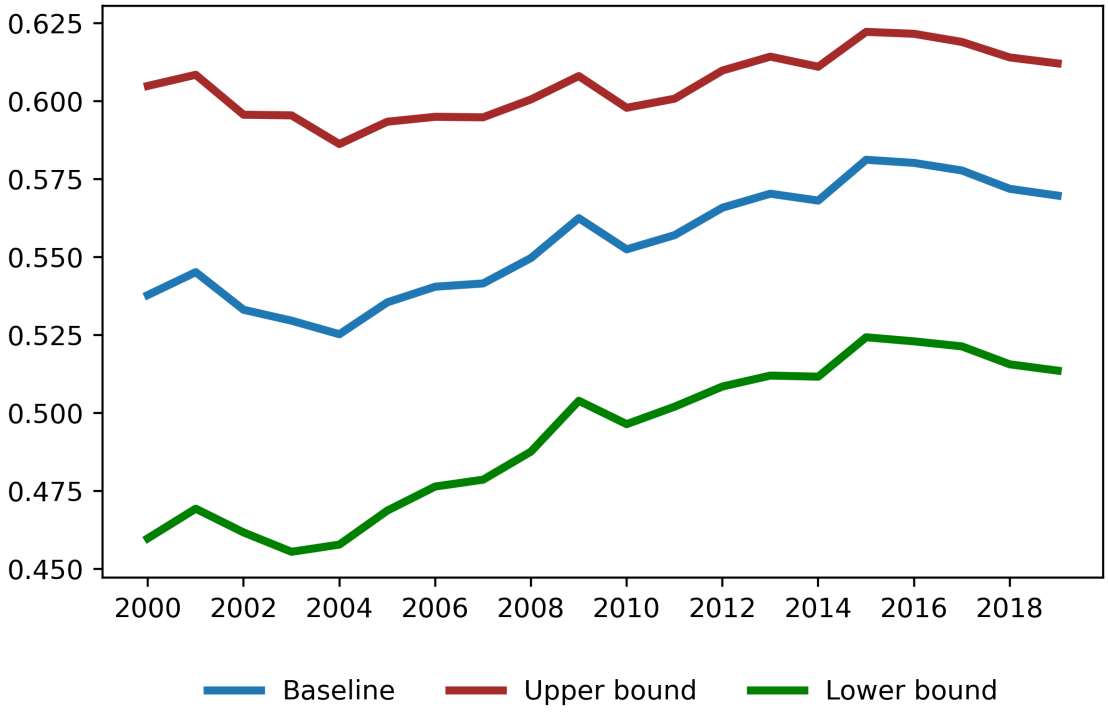

Figure 5: Series of the labor income share LS.

As robustness exercises, we apply our methodology using these two alternative labor income share estimates. For each new series, we first recalculate the capital cost share, which will be higher for lower labor income shares, and then re-calibrate α following the procedure outlined in Section 4.2. Using the upper-bound (lower-bound) LS series, we find α to be 0.37 (0.41). Nonetheless, the average markup $\mu = \frac{1-\alpha}{LS}$ decreases as the labor income share LS increases, which is not unexpected.[17] Finally, for each alternative series, we use the new α and LS values to re-estimate the other parameters, including β.

The results shown in Table 4 for the upper-bound LS series continue to support that the technology component $\overline{A}$ grows more steadily than the TFP $\overline{A}\Omega$ itself, with allocative efficiency Ω remaining an important driver of TFP cycles. However, the cyclical role of technology becomes significantly more important in this case. Specifically, while the high TFP growth between 2007 and 2016 is largely attributed to Ω, the greater growth from 2003 to 2007 is primarily driven by $\overline{A}$. Over the 2003–2016 period as a whole, we find nearly equal contributions from these two components.[18] This increased importance of the technology component arises because it be-

[17] Since $\alpha = \frac{Kr}{Kr+Lw} = \frac{KS}{KS+LS}$, where KS represents the capital share of national income, we have $\mu = \frac{1-\alpha}{LS} = \frac{1-\frac{KS}{KS+LS}}{LS} = \frac{1}{KS+LS}$.

[18] From 2003 to 2016, the annual growth of TFP $\overline{A}\Omega$ was 1.42%, with $\overline{A}$ growing at 1.23% and Ω at 0.18%.

comes more pro-cyclical, as allocative efficiency becomes less pro-cyclical, due to two reasons. On the one hand, the labor share is highly positively correlated with GDP, with a correlation of 0.88. On the other hand, a higher LS results in a smaller μ, and under these conditions, the impact of changes in μ on allocative efficiency Ω is smaller, as illustrated in Figure 1.

By analogous reasoning, one should expect a more pro-cyclical allocative efficiency Ω for the lower-bound LS series, with Ω playing an even greater role in explaining TFP cycles. The results shown in Table 4 are consistent with this expectation. Indeed, Ω is so cyclical that the residual $\overline{A}$ becomes significantly more volatile and, notably, countercyclical. For example, between 2000–2003 and 2003–2007, the growth of the technology frontier $\overline{A}$ decreased while GDP and TFP accelerated, which appears counterintuitive. This suggests the naïve approach to computing the labor income share is inappropriate for a developing economy like Brazil, as argued by Gollin (2002).

In short, the results change qualitatively only under the unreasonable assumption that no mixed income is attributed to labor. Allocating all mixed income to labor increases the variance of the technology component, but it still grows more steadily than the TFP itself, with allocative efficiency remaining a key driver of TFP cycles.

6.4 Zipf's law calibration

Until now, we have always quantified the model under the assumption that firm productivity A is Pareto distributed. While this assumption is relatively standard in the literature, assessing its reasonableness is challenging since firm productivity is rarely observable. What can be more easily observed is the distribution of firm size, which typically follows a distributional power law known as Zipf's law.[19] Formally, under this "law," $P(s \geq S) = (\underline{S}/S)^k$ for some measure of firm size $s \geq \underline{S}$, with $k \approx 1$. Empirical evidence supporting this claim has been found across several different countries, with firm size measured by the number of employees, sales, income, total assets, and equity plus debt (Okuyama et al. 1999, Axtell 2001, Fujiwara et al. 2004, Luttmer 2007, Gabaix and Landier 2008, Di Giovanni et al. 2011, and Di Giovanni and Levchenko 2013). Specifically in Brazil, Da Silva et al. (2018) find support for Zipf's law among the 1,000 largest firms by net revenue in 2015. Additionally, Santos and Cajueiro (2024) evaluate the distribution of firm size by the number of employees using CEMPRE data. Remarkably, they find Zipf's law provides a very good, though not perfect, approximation to data for each year between 1996 and 2020, both at the economy-wide level and within the agriculture, industry, and services sectors.

Given this scenario, instead of choosing a density for A, we now impose a distribution for firm market share $s(A)$.[20] As before, we opt to use a continuous distribution, consistent with

[19] Power laws emerge in various domains within economics and finance. See Gabaix (2009, 2016) for a review.

[20] In monopolistic competition models like Melitz (2003), supposing firm productivity is Pareto distributed results in a distributional power law of firm size (Di Giovanni et al. 2011). This does not hold for the Cournot model of Martinez and Santos (2024).

the continuous model of Martinez and Santos (2024). However, we cannot assume market share follows a non-truncated Pareto distributed with shape parameter $k \approx 1$, when Zipf's law would hold over the entire support. On the one hand, a truncated distribution is necessary because market share is bounded. On the other hand, since $s(\underline{A}) = 0$, the support of the market share distribution is not strictly greater than 0. Under such circumstances, we assume the market share $s(A)$ follows a truncated Lomax distribution, which is a special case of the truncated Pareto type II. Specifically, we assume $\tilde{s}(A) \equiv 1 - \underline{A}/A = \frac{s(A)}{\eta/q} \in \left[0, \tilde{s}(\overline{A})\right] = \left[0, 1 - \tilde{A}^{-1}\right]$ is truncated Lomax distributed with shape parameter $k \neq 0$ and scale parameter $\lambda > 0$, or equivalently, $(\tilde{s}(A) + \lambda) \in [\lambda, \tilde{s}(\overline{A}) + \lambda]$ is truncated Pareto distributed with shape parameter $k \neq 0$. Therefore, for $\lambda \approx 0$, firm market share is approximately truncated Pareto distributed. If we further assume $k \approx 1$, the distribution aligns with Zipf's law predictions, particularly away from the bounds of the support (see Appendix C.1 for a discussion).

We left the details to Appendix C, but we essentially follow the same two-stage procedure outlined in Section 3.3 to quantify the model. In the first stage, given k and λ, we gauge $\underline{A}$ and $\overline{A}$ by matching aggregate TFP $\overline{A}\Omega$ and average markup μ. In the second stage, we set $k \approx 1$ and search for the time-invariant λ that minimizes the distance to the normalized $N_a HHI_L$. Similar to the baseline Pareto case, TFP data are not required to estimate Ω, not even through λ. They are used solely to pin down $\underline{A}$ and $\overline{A}$. Hence, as before, the residual in this model is not the TFP $\overline{A}\Omega$ itself, but rather only its technology component $\overline{A}$.

Table 4 presents the TFP decomposition under the new distribution for $k = 0.5, 1, 1.5$. The results are practically identical to those of the baseline model across all three shape parameters. The estimated scale parameter λ is 0.55, 0.76, and 0.97 for k equal to 0.5, 1, and 1.5, respectively. Thus, the choice of k does not seem to be crucial, as varying k affects the calibrated λ in the second stage, leaving the main model results basically unchanged.[21]

7 Conclusion

This paper employs the Cournot model of Martinez and Santos (2024) to decompose Brazilian TFP into technology and allocative efficiency components from 2000 to 2019. Over these two decades, we observe an overall improvement in allocative efficiency, reflecting an increase in the labor income share and a corresponding decrease in the average markup. Additionally, we find the cycles in TFP are predominantly driven by allocative efficiency, with the mid-2000s economic boom primarily attributed to efficiency gains. In contrast, the technology component grows more steadily, suggesting it reflects structural characteristics of the economy. Therefore, since allocative efficiency cannot increase or decrease indefinitely, the technology growth rate, of around 0.9% per year, can be interpreted as the current long-run growth rate of Brazilian

[21] When seeking both $k \neq 0$ and $\lambda > 0$ in the second stage, we find very high values: $k \approx 212$ and $\lambda \approx 90$. Despite these high values, the TFP decomposition remains practically identical to the baseline model, further confirming this intuition.

TFP.

The main conclusions are robust to using conservatively a uniform distribution, when the model quantification requires *only* macroeconomic data. They are also robust to adopting the standard $\alpha = 1/3$ or $\alpha = 0.41$ instead of our baseline calibration of $\alpha = 0.39$. Using a higher labor income share, with all mixed income allocated to labor, does not substantially alter our main conclusions either. Finally, the results remain unchanged when we assume the distribution of firm market share is consistent with Zipf's law rather than imposing a productivity density.

Appendices

A Derivation of two concentration measures

Relying on the results of Martinez and Santos (2024), we derive expressions for two concentration measures. First, the Herfindahl–Hirschman index (HHI) of the labor market, defined as $HHI_L \equiv \sum_{i=1}^{N}(L_i/L)^2$, where L_i is the labor employed by firm $i \in \{1, 2, ..., N\}$ and $L \equiv \sum_{i=1}^{N} L_i$. Second, the HHI of the product market, defined as $HHI_s \equiv \sum_{i=1}^{N} s(A_i)^2$, where $s(A_i)$ is the market share of an active firm with productivity A_i. We begin with their baseline model, which we employ in the main text, but we also consider the two model extensions presented in Martinez and Santos (2024).

A.1 Baseline model

Martinez and Santos (2024) derive the following results for their discrete model:

$$\theta_i \equiv \theta_{Li} = \theta_{Ki} = \overline{A}\Omega \frac{s(A_i)}{A_i} \tag{A.1}$$

$$s(A_i) \approx \eta\,(1 - \underline{A}/A_i) \tag{2}$$

$$\eta \approx \frac{1}{N_a\,[1 - \mathrm{E}_a\,(\underline{A}/A)]} \tag{3}$$

$$\Omega \approx \frac{\mathrm{E}_a\left[(\underline{A}/\overline{A})(1 - \underline{A}/A)\right]}{\mathrm{E}_a\left[(\underline{A}/A)(1 - \underline{A}/A)\right]} \tag{5}$$

$$\mu \approx \frac{\overline{A}\Omega}{\underline{A}}, \tag{6}$$

where $\theta_{Li} \equiv L_i/L$ and $\theta_{Ki} \equiv K_i/K$, with K_i being the capital stock of firm i and $K \equiv \sum_{i=1}^{N} K_i$. Aggregate TFP is denoted by $\overline{A}\Omega$, with Ω being a measure of allocative efficiency and $\overline{A}$ the productivity of the most efficient firm. Moreover, $\underline{A}$ is the lowest productivity level among active firms, η is the absolute value of the price elasticity of demand, N_a is the number of active firms, and $\mathrm{E}_a\,(h(A))$ is the expected value of a function h over active firms under the empirical distribution. Finally, being μ_i the markup of firm i, w the wage, and r the rental cost of capital, $\mu \equiv \sum_{i=1}^{N} \left(\frac{L_i w + K_i r}{Lw + Kr}\right) \mu_i$ is the cost-weighted average of firm-level markups.

Using these results, let us derive expressions for the two measures of concentration presented earlier. First, the HHI of the labor market $HHI_L \equiv \sum_{i=1}^{N} \theta_{Li}^2$. Plugging (A.1) into this definition and using (2) and (3),

$$HHI_L = \sum_{i=1}^{N} \left[\overline{A}\Omega \frac{s(A_i)}{A_i}\right]^2 \approx \left[\frac{\Omega(\overline{A}/\underline{A})}{1 - \mathrm{E}_a\,(\underline{A}/A)}\right]^2 \frac{\mathrm{E}_a\left[(\underline{A}/A)^2\,(1 - \underline{A}/A)^2\right]}{N_a}$$

$$
\begin{aligned}
N_a HHI_L \approx & \Omega^2 \frac{\mathrm{E}_a\left[(\underline{A}/A)^2\left(1-\underline{A}/A\right)^2\right]}{\left\{\mathrm{E}_a\left[(\underline{A}/\overline{A})\left(1-\underline{A}/A\right)\right]\right\}^2} \\
N_a HHI_L \approx & \frac{\mathrm{E}_a\left[(\underline{A}/A)^2\left(1-\underline{A}/A\right)^2\right]}{\left\{\mathrm{E}_a\left[(\underline{A}/A)(1-\underline{A}/A)\right]\right\}^2},
\end{aligned} \tag{7}
$$

where in the last line we use (5). Second, the HHI of the product market $HHI_s \equiv \sum_{i=1}^{N} s(A_i)^2$. Plugging (2) and (3) into it, one gets

$$
N_a HHI_s \approx \frac{\mathrm{E}_a\left[\left(1-\underline{A}/A\right)^2\right]}{\left[\mathrm{E}_a\left(1-\underline{A}/A\right)\right]^2} \approx \frac{1-1/\mu}{1-\mathrm{E}_a\left(\underline{A}/A\right)}, \tag{8}
$$

where in the last part we use (5) and (6), since, from these equations,

$$
\begin{aligned}
1-\frac{1}{\mu} \approx & 1-\frac{\underline{A}}{\overline{A}\Omega} \approx 1-\frac{\mathrm{E}_a\left[(\underline{A}/A)(1-\underline{A}/A)\right]}{1-\mathrm{E}_a\left(\underline{A}/A\right)} \\
1-\frac{1}{\mu} \approx & \frac{1-2\mathrm{E}_a\left(\underline{A}/A\right)+\mathrm{E}_a\left[(\underline{A}/A)^2\right]}{1-\mathrm{E}_a\left(\underline{A}/A\right)} = \frac{\mathrm{E}_a\left[(1-\underline{A}/A)^2\right]}{1-\mathrm{E}_a\left(\underline{A}/A\right)}.
\end{aligned} \tag{A.2}
$$

In another version of their model, Martinez and Santos (2024) consider a continuum of firms indexed by $i \in [0, N]$. In this case, the results shown at the beginning of this section would still be valid, but now holding *exactly*, if (i) η is replaced by η/q, with $q \in (0, 1]$ being the marginal effect of increasing a firm's output on aggregate output considered by each firm, and (ii) integrals are used instead of sums (e.g., $Y \equiv \int_0^N Y_i di$). Given that, Equations (7) and (8) are also valid for the continuous model, but in this case holding *exactly*. Naturally, the measures of concentration should be defined accordingly, with $HHI_L \equiv \int_0^N \theta_{Li}^2 di$ and $HHI_s \equiv \int_0^N s(A_i)^2 di$.

A.2 Model extensions

Martinez and Santos (2024) discuss two model extensions. In the first extension, they go beyond the Cobb-Douglas production function, considering an arbitrary well-behaved production function with M factors of production, provided it exhibits (i) constant returns to scale and (ii) Hicks-neutral productivity shifter. In this case, they show the baseline Equations (A.1), (2), (3), (5), and (6) are still valid, implying (7) and (8) continue to hold (exactly for a continuum of firms).[22] In the second extension, they add firm-specific wedges as a new source of firm heterogeneity, considering firm-specific tax rate over revenue $\tau_i = \tau(A_i)$. In this case, for a discrete number of firms,

$$
\theta_i \equiv \theta_{Li} = \theta_{Ki} = \overline{A}\Omega \frac{s(B_i)}{A_i} \tag{A.1"}
$$

$$
s(B_i) \approx \eta\left(1-\underline{B}/B_i\right) \tag{2"}
$$

[22] Naturally, for HHI_L to make sense, labor should be one of the factors of production.

$$\eta \approx \frac{1}{N_a \left[1 - \mathrm{E}_a \left(\underline{B}/B\right)\right]} \tag{3"}$$

$$\Omega \approx \frac{\mathrm{E}_a \left[(\underline{A}/\overline{A})(1 - \underline{B}/B)\right]}{\mathrm{E}_a \left[(\underline{A}/A)(1 - \underline{B}/B)\right]} \tag{5"}$$

$$\mu \approx \frac{\overline{A}\Omega}{\underline{B}} \left(1 - \tilde{\tau}\right), \tag{6"}$$

where $s(B_i)$ is the market share of a firm with adjusted productivity $B_i \equiv A_i \left(1 - \tau(A_i)\right)$, $\underline{B}$ is the lowest level of the adjusted productivity B_i among active firms, and $\tilde{\tau} \equiv \sum_{i=1}^{N} s(B_i)\tau(A_i)$ is the sales-weighted average tax rate. As a result, plugging (A.1") into $HHI_L \equiv \sum_{i=1}^{N} \theta_{Li}^2$ and using (2") and (3"),

$$N_a HHI_L \approx (\overline{A}\Omega)^2 \frac{E_a \left[\left((1/A) - \underline{B}/(A \times B)\right)^2\right]}{\left[1 - \mathrm{E}_a \left(\underline{B}/B\right)\right]^2} = \left(\frac{\overline{A}\Omega}{\underline{A}}\right)^2 \frac{E_a \left[(\underline{A}/A)^2 (1 - \underline{B}/B)^2\right]}{\left[1 - \mathrm{E}_a \left(\underline{B}/B\right)\right]^2}$$

$$N_a HHI_L \approx \frac{E_a \left[(\underline{A}/A)^2 (1 - \underline{B}/B)^2\right]}{\left\{\mathrm{E}_a \left[(\underline{A}/A)(1 - \underline{B}/B)\right]\right\}^2}, \tag{7"}$$

where in the last line we use (5"). Finally, plugging (2") and (3") into $HHI_s \equiv \sum_{i=1}^{N} s_i^2$,

$$N_a HHI_s \approx \frac{\mathrm{E}_a \left[(1 - \underline{B}/B)^2\right]}{\left[\mathrm{E}_a \left(1 - \underline{B}/B\right)\right]^2}. \tag{8"}$$

By analogous reasoning to that employed previously for the baseline model, Equations (7") and (8") would be *exactly* valid with a continuum of firms. As before, in this case, one should define $HHI_L \equiv \int_0^N \theta_{Li}^2 di$ and $HHI_s \equiv \int_0^N s(A_i)^2 di$.

B Conditions for the first-stage algorithm to work properly

Martinez and Santos (2024) establish necessary and sufficient conditions for the first-stage algorithm to function properly, ensuring an exact match of both target moments. Initially, they derive some general results by examining an arbitrary truncated distribution, with the only requirement being that its density can be expressed as an upper truncation of another distribution. These general findings provide a framework for establishing conditions applicable to any such distribution. Martinez and Santos (2024) utilize this framework to assess the case where firm productivity is truncated Pareto distributed. Here, we apply it to the case where firm market share follows a truncated Lomax distribution, demonstrating the conditions under which (10) implicitly defines $\tilde{A} \equiv \overline{A}/\underline{A}$ as a well-defined function of μ.

In the following, consider μ as given in (10) or, equivalently,

$$\mu = \frac{\mathrm{E}_a\left(1 - \underline{A}/A\right)}{\mathrm{E}_a\left(1 - \underline{A}/A\right) - \mathrm{E}_a\left[(1 - \underline{A}/A)^2\right]}, \tag{10}$$

where $\mathrm{E}_a\left(h(A)\right) \equiv \mathrm{E}\left(h(A) | \underline{A} \leq A \leq \overline{A}\right)$ for any function h.

B.1 Arbitrary distribution

Assume $A \in [\underline{\underline{A}}, \overline{A}]$ is a continuous variable, $0 < \underline{\underline{A}} < \overline{A} < +\infty$, whose density and cumulative distribution function are g and G, respectively. Let $\tilde{g}(A) \equiv \frac{g(A)}{1-G(\underline{A})} > 0$, $\underline{A} \in (\underline{\underline{A}}, \overline{A})$, the density function of $A \in [\underline{A}, \overline{A}]$, with cumulative distribution $\tilde{G}$. Let $\hat{g}$ be another density of A, but defined over the support $A \in [\underline{A}, A_h]$, $A_h > \overline{A}$, possibly with $A_h \to +\infty$. This density does not depend on $\overline{A}$ and has cumulative distribution function $\hat{G}$. Moreover, it satisfies $\tilde{g}(A) = \frac{\hat{g}(A)}{\hat{G}(\overline{A})}$, meaning $\tilde{g}$ is an upper truncation of $\hat{g}$.

Proposition B.1 *$\overline{A}$, $\overline{A} > \underline{A}$, is a continuous, strictly increasing, and well-defined function of μ if and only if $\mu \in \left(1, \lim_{\overline{A}\to+\infty} \mu\right)$.*

Proof. See Martinez and Santos (2024). ■

B.2 Lomax distribution of firm market share

Let $\tilde{s}(A) \equiv 1 - \underline{A}/A$ for $A \in [\underline{A}, \overline{A}] \in (0, +\infty)$, with $\tilde{A} \equiv \overline{A}/\underline{A} > 1$. Assume $\tilde{s}(A) \in [0, \tilde{s}(\overline{A})] = [0, 1 - \tilde{A}^{-1}]$ is truncated Lomax distributed with shape parameter $k \neq 0$ and scale parameter $\lambda > 0$ or, equivalently, $(\tilde{s}(A) + \lambda) \in [\lambda, \tilde{s}(\overline{A}) + \lambda]$ is truncated Pareto distributed with the same parameter $k \neq 0$. Hence, the density of $\tilde{s}(A)$ is $\tilde{g}_s(\tilde{s}(A)) = k\left[\frac{\lambda^k(\tilde{s}(\overline{A})+\lambda)^k}{(\tilde{s}(\overline{A})+\lambda)^k - \lambda^k}\right](\tilde{s}(A) + \lambda)^{-k-1} = k\left(\frac{\lambda^k S^k}{S^k - 1}\right)(\tilde{s}(A) + \lambda)^{-k-1}$, where $S \equiv \frac{\tilde{s}(\overline{A})}{\lambda} + 1$ is a function of $\tilde{A}$ and λ. Denote by $\tilde{G}_s$ the cumulative distribution function of $\tilde{s}(A)$. In the following, let $\overline{\mu} \equiv \lim_{\overline{A}\to+\infty} \mu$.

Proposition B.2 *For $k \neq 0$, $\lambda > 0$, and $j \in \mathbb{N} \setminus \{0\}$,*

$$\mathrm{E}_a\left[(\tilde{s}(A)+\lambda)^j\right] = \begin{cases} \frac{k\lambda^j}{j-k}\left(\frac{S^j-S^k}{S^k-1}\right) & \text{, if } j \neq k \\ k\lambda^k\left(\frac{S^k \ln S}{S^k-1}\right) & \text{, if } j = k \end{cases}.$$

Proof. Let $k \neq 0$, $\lambda > 0$, and $j \in \mathbb{N} \setminus \{0\}$. From the truncated Lomax density, if $j \neq k$,

$$\begin{aligned}
\mathrm{E}_a\left[(\tilde{s}(A)+\lambda)^j\right] =& k\left(\frac{\lambda^k S^k}{S^k-1}\right)\int_0^{\tilde{s}(\overline{A})}(s+\lambda)^{j-k-1}ds = k\left(\frac{\lambda^k S^k}{S^k-1}\right)\left[\frac{(\tilde{s}(\overline{A})+\lambda)^{j-k}-\lambda^{j-k}}{j-k}\right] \\
\mathrm{E}_a\left[(\tilde{s}(A)+\lambda)^j\right] =& k\left(\frac{\lambda^k S^k}{S^k-1}\right)\left[\frac{S^{j-k}-1}{(j-k)\lambda^{k-j}}\right] = \frac{k\lambda^j}{j-k}\left(\frac{S^j-S^k}{S^k-1}\right),
\end{aligned}$$

while, if $j = k$, $\mathrm{E}_a\left[(\tilde{s}(A)+\lambda)^j\right] = k\left(\frac{\lambda^k S^k}{S^k-1}\right)\left[\ln(\tilde{s}(\overline{A})+\lambda)-\ln(\lambda)\right] = k\lambda^k\left(\frac{S^k \ln S}{S^k-1}\right)$. ■

Proposition B.3 *For $\lambda > 0$, $\mu = \begin{cases} \frac{k(S-1)-(S^k-1)}{\left(1+\frac{2\lambda}{2-k}\right)\left[k(S-1)-(S^k-1)\right]-\frac{\lambda k(1-k)}{2-k}(S-1)^2} & \text{, if } k \neq 0,1,2 \\ \frac{S\ln S-(S-1)}{(1+2\lambda)[S\ln S-(S-1)]-\lambda(S-1)^2} & \text{, if } k = 1 \\ \frac{(S-1)^2}{2(1+2\lambda)S(S-1)-2\lambda S^2\ln S-(1+\lambda)(S^2-1)} & \text{, if } k = 2 \end{cases}$.*

Proof. Let $\lambda > 0$. Initially, note Equation (10) can be rewritten as

$$\begin{aligned}
\mu =& \frac{\mathrm{E}_a\left(1-\underline{A}/A\right)}{\mathrm{E}_a\left(1-\underline{A}/A\right)-\mathrm{E}_a\left[(1-\underline{A}/A)^2\right]} = \frac{\mathrm{E}_a\left(\tilde{s}(A)\right)}{\mathrm{E}_a\left(\tilde{s}(A)\right)-\mathrm{E}_a\left[\tilde{s}(A)^2\right]} \\
\mu =& \frac{\mathrm{E}_a\left(\tilde{s}(A)+\lambda\right)-\lambda}{\mathrm{E}_a\left(\tilde{s}(A)\right)-\mathrm{E}_a\left[\left(\tilde{s}(A)+\lambda\right)^2\right]+\lambda^2+2\lambda\mathrm{E}_a\left[\tilde{s}(A)\right]} \\
\mu =& \frac{\mathrm{E}_a\left(\tilde{s}(A)+\lambda\right)-\lambda}{(1+2\lambda)\mathrm{E}_a\left(\tilde{s}(A)+\lambda\right)-\lambda(1+2\lambda)-\mathrm{E}_a\left[\left(\tilde{s}(A)+\lambda\right)^2\right]+\lambda^2} \\
\mu =& \frac{\mathrm{E}_a\left(\tilde{s}(A)+\lambda\right)-\lambda}{(1+2\lambda)\mathrm{E}_a\left(\tilde{s}(A)+\lambda\right)-\mathrm{E}_a\left[\left(\tilde{s}(A)+\lambda\right)^2\right]-\lambda(1+\lambda)},
\end{aligned}$$

since $\tilde{s}(A) \equiv 1-\underline{A}/A$, where $\mathrm{E}_a\left[h(\tilde{s}(A))\right] = \int_{\tilde{s}(\underline{A})}^{\tilde{s}(\overline{A})} h(s)\tilde{g}_s(s)ds$ for a function h.

Therefore, if $k = 1$, using Proposition B.2 one can see that

$$\begin{aligned}
\mu =& \frac{\lambda\left(\frac{S\ln S}{S-1}\right)-\lambda}{(1+2\lambda)\lambda\left(\frac{S\ln S}{S-1}\right)-\lambda^2\left(\frac{S^2-S}{S-1}\right)-\lambda(1+\lambda)} \\
\mu =& \frac{S\ln S-(S-1)}{(1+2\lambda)S\ln S-\lambda S(S-1)-(1+2\lambda-\lambda)(S-1)} \\
\mu =& \frac{S\ln S-(S-1)}{(1+2\lambda)\left[S\ln S-(S-1)\right]-\lambda(S-1)^2}.
\end{aligned}$$

If $k = 2$, from Proposition B.2,

$$\begin{aligned}
\mu =& \frac{2\lambda\left(\frac{S^2-S}{S^2-1}\right) - \lambda}{(1+2\lambda)2\lambda\left(\frac{S^2-S}{S^2-1}\right) - 2\lambda^2\left(\frac{S^2\ln S}{S^2-1}\right) - \lambda(1+\lambda)} \\
\mu =& \frac{2S(S-1) - (S^2-1)}{2(1+2\lambda)S(S-1) - 2\lambda S^2\ln S - (1+\lambda)(S^2-1)} \\
\mu =& \frac{(S-1)^2}{2(1+2\lambda)S(S-1) - 2\lambda S^2\ln S - (1+\lambda)(S^2-1)}.
\end{aligned}$$

Finally, if $k \neq 0, 1, 2$,

$$\begin{aligned}
\mu =& \frac{\frac{k\lambda}{1-k}\left(\frac{S-S^k}{S^k-1}\right) - \lambda}{(1+2\lambda)\frac{k\lambda}{1-k}\left(\frac{S-S^k}{S^k-1}\right) - \frac{k\lambda^2}{2-k}\left(\frac{S^2-S^k}{S^k-1}\right) - \lambda(1+\lambda)} \\
\mu =& \frac{\frac{k}{1-k}(S-S^k) - (S^k-1)}{(1+2\lambda)\frac{k}{1-k}(S-S^k) - \lambda\frac{k}{2-k}(S^2-S^k) - (1+2\lambda-\lambda)(S^k-1)} \\
\mu =& \frac{\frac{k}{1-k}(S-S^k) - (S^k-1)}{(1+2\lambda)\left[\frac{k}{1-k}(S-S^k) - (S^k-1)\right] - \lambda\left[\frac{k}{2-k}(S^2-S^k) - (S^k-1)\right]} \\
\mu =& \frac{\frac{k(S-1)-(S^k-1)}{1-k}}{(1+2\lambda)\left[\frac{k(S-1)-(S^k-1)}{1-k}\right] - \frac{\lambda}{2-k}\left[k(S^2-1) - 2(S^k-1)\right]} \\
\mu =& \frac{k(S-1) - (S^k-1)}{(1+2\lambda)\left[k(S-1) - (S^k-1)\right] - \frac{\lambda(1-k)}{2-k}\left[2k(S-1) - 2(S^k-1) + k(S-1)^2\right]} \\
\mu =& \frac{k(S-1) - (S^k-1)}{\left[(1+2\lambda) - \frac{2\lambda(1-k)}{2-k}\right]\left[k(S-1) - (S^k-1)\right] - \frac{\lambda(1-k)}{2-k}\left[k(S-1)^2\right]} \\
\mu =& \frac{k(S-1) - (S^k-1)}{\left(1+\frac{2\lambda}{2-k}\right)\left[k(S-1) - (S^k-1)\right] - \frac{\lambda k(1-k)}{2-k}(S-1)^2},
\end{aligned}$$

where we once again use Proposition B.2. ■

Proposition B.4 *For* $\lambda > 0$, $\overline{\mu} = \begin{cases} \frac{1}{\left(1+\frac{2\lambda}{2-k}\right) - \frac{k(1-k)/(2-k)}{k-\lambda\left[\left(\frac{\lambda+1}{\lambda}\right)^k - 1\right]}} & \text{, if } k \neq 0, 1, 2 \\ \frac{1}{(1+2\lambda) - \left[(\lambda+1)\ln\left(\frac{\lambda+1}{\lambda}\right) - 1\right]^{-1}} & \text{, if } k = 1 \\ \frac{1}{(1+2\lambda)(\lambda+1) - 2\lambda(\lambda+1)^2\ln\left(\frac{\lambda+1}{\lambda}\right)} & \text{, if } k = 2 \end{cases}$.

Proof. Let $\lambda > 0$. Since $S \equiv \frac{\tilde{s}(\overline{A})}{\lambda} + 1$ and $\tilde{s}(A) \equiv 1 - \underline{A}/A_i$, $S = \frac{1-\tilde{A}^{-1}}{\lambda} + 1$. Hence, $S \to \frac{\lambda+1}{\lambda}$ as $\overline{A} \to +\infty$, implying $\overline{\mu} \equiv \lim_{\overline{A}\to+\infty}\mu = \lim_{S\to\frac{\lambda+1}{\lambda}}\mu$. As a result, if $k = 1$, from Proposition B.3,

$$\lim_{\overline{A}\to+\infty}\mu = \lim_{S\to\frac{\lambda+1}{\lambda}}\frac{S\ln S - (S-1)}{(1+2\lambda)\left[S\ln S - (S-1)\right] - \lambda(S-1)^2}$$

$$\lim_{\overline{A}\to+\infty}\mu = \frac{(\lambda+1)\ln\left(\frac{\lambda+1}{\lambda}\right)-1}{(1+2\lambda)\left[(\lambda+1)\ln\left(\frac{\lambda+1}{\lambda}\right)-1\right]-1} = \frac{1}{(1+2\lambda)-\left[(\lambda+1)\ln\left(\frac{\lambda+1}{\lambda}\right)-1\right]^{-1}}.$$

If $k=2$, using Proposition B.3,

$$\begin{aligned}
\lim_{\overline{A}\to+\infty}\mu &= \lim_{S\to\frac{\lambda+1}{\lambda}} \frac{(S-1)^2}{2(1+2\lambda)S(S-1)-2\lambda S^2\ln S-(1+\lambda)(S^2-1)} \\
\lim_{\overline{A}\to+\infty}\mu &= \frac{\frac{1}{\lambda^2}}{2(1+2\lambda)\left(\frac{\lambda+1}{\lambda}\right)\left(\frac{1}{\lambda}\right)-2\lambda\left(\frac{\lambda+1}{\lambda}\right)^2\ln\left(\frac{\lambda+1}{\lambda}\right)-(1+\lambda)\left(\frac{1+2\lambda}{\lambda}\right)\left(\frac{1}{\lambda}\right)} \\
\lim_{\overline{A}\to+\infty}\mu &= \frac{1}{(1+2\lambda)(\lambda+1)-2\lambda(\lambda+1)^2\ln\left(\frac{\lambda+1}{\lambda}\right)}.
\end{aligned}$$

Finally, if $k\neq 0,1,2$,

$$\begin{aligned}
\lim_{\overline{A}\to+\infty}\mu &= \lim_{S\to\frac{\lambda+1}{\lambda}} \frac{k(S-1)-(S^k-1)}{\left(1+\frac{2\lambda}{2-k}\right)\left[k(S-1)-(S^k-1)\right]-\frac{\lambda k(1-k)}{2-k}(S-1)^2} \\
\lim_{\overline{A}\to+\infty}\mu &= \frac{1}{\left(1+\frac{2\lambda}{2-k}\right)-\frac{\left[\frac{\lambda k(1-k)}{2-k}\right]\frac{1}{\lambda^2}}{\frac{k}{\lambda}-\left[\left(\frac{\lambda+1}{\lambda}\right)^k-1\right]}} = \frac{1}{\left(1+\frac{2\lambda}{2-k}\right)-\frac{k(1-k)/(2-k)}{k-\lambda\left[\left(\frac{\lambda+1}{\lambda}\right)^k-1\right]}},
\end{aligned}$$

where we again use Proposition B.3. ■

Proposition B.5 *For $\lambda>0$ and $k\in(0,2]$, $\frac{\partial\overline{\mu}}{\partial\lambda}>0$.*

Proof. Let $\lambda>0$. It is sufficient to show $\frac{\partial(1/\overline{\mu})}{\partial\lambda}<0$ for $k\in(0,2]$. If $k=1$, from Proposition B.4,

$$\begin{aligned}
\frac{\partial(1/\overline{\mu})}{\partial\lambda} &= \frac{\partial\left[(1+2\lambda)-\left[(\lambda+1)\ln\left(\frac{\lambda+1}{\lambda}\right)-1\right]^{-1}\right]}{\partial\lambda} \\
\frac{\partial(1/\overline{\mu})}{\partial\lambda} &= 2+\frac{\ln\left(\frac{\lambda+1}{\lambda}\right)+\lambda\left(-\frac{1}{\lambda^2}\right)}{\left[(\lambda+1)\ln\left(\frac{\lambda+1}{\lambda}\right)-1\right]^2} = \frac{2\left[\left(\frac{\lambda+1}{\lambda}\right)\ln\left(\frac{\lambda+1}{\lambda}\right)-\frac{1}{\lambda}\right]^2+\frac{1}{\lambda^2}\ln\left(\frac{\lambda+1}{\lambda}\right)-\frac{1}{\lambda^3}}{\lambda^{-2}\left[(\lambda+1)\ln\left(\frac{\lambda+1}{\lambda}\right)-1\right]^2}.
\end{aligned}$$

Being $y\equiv\frac{\lambda+1}{\lambda}\to\lambda=\frac{1}{y-1}$,

$$\begin{aligned}
f(y) &\equiv 2\left[\left(\frac{\lambda+1}{\lambda}\right)\ln\left(\frac{\lambda+1}{\lambda}\right)-\frac{1}{\lambda}\right]^2+\frac{1}{\lambda^2}\ln\left(\frac{\lambda+1}{\lambda}\right)-\frac{1}{\lambda^3} \\
f(y) &= 2\left[y\ln y-(y-1)\right]^2+(y-1)^2\ln y-(y-1)^3\to f(1)=0
\end{aligned}$$

$$\begin{aligned}
f'(y) &= 4\left[y\ln y-(y-1)\right]\ln y+2(y-1)\ln y+\frac{(y-1)^2}{y}-3(y-1)^2 \\
f'(y) &= 2\left[2y\ln y-(y-1)\right]\ln y+(y-1)^2\left(\frac{1}{y}-3\right)\to f'(1)=0
\end{aligned}$$

$$
\begin{aligned}
f''(y) =& 2\left[2\ln y - \left(\frac{y-1}{y}\right)\right] + 2\left(2\ln y + 1\right)\ln y + 2(y-1)\left(\frac{1}{y} - 3\right) + (y-1)^2\left(-\frac{1}{y^2}\right) \\
f''(y) =& \ln y\left(4\ln y + 6\right) - \left(\frac{y-1}{y}\right)^2 - 6(y-1) \rightarrow f''(1) = 0
\end{aligned}
$$

$$
\begin{aligned}
f'''(y) =& \left(\frac{4\ln y + 6}{y}\right) + 4\frac{\ln y}{y} - 2\left(\frac{y-1}{y}\right)\left(\frac{1}{y^2}\right) - 6 \\
f'''(y) =& 2y^{-3}\left[4y^2\ln y - (y-1) + 3y^2 - 3y^3\right]
\end{aligned}
$$

$$
\begin{aligned}
g(y) \equiv& 4y^2\ln y - (y-1) + 3y^2 - 3y^3 \rightarrow g(1) = 0 \\
g'(y) =& 8y\ln y + 4y - 1 + 6y - 9y^2 = 8y\ln y + 10y - 9y^2 - 1 \rightarrow g'(1) = 0 \\
g''(y) =& 8\ln y + 8 + 10 - 18y = 8\ln y - 18y + 18 \rightarrow g''(1) = 0 \\
g'''(y) =& 8y^{-1} - 18.
\end{aligned}
$$

Since $\lambda > 0 \rightarrow y > 1$, $g'''(y) < 0 \xrightarrow{g''(1)=0} g''(y) < 0 \xrightarrow{g'(1)=0} g'(y) < 0 \xrightarrow{g(1)=0} g(y) < 0 \rightarrow f'''(y) < 0 \xrightarrow{f''(1)=0} f''(y) < 0 \xrightarrow{f'(1)=0} f'(y) < 0 \xrightarrow{f(1)=0} f(y) < 0$. Thus, $\frac{\partial(1/\overline{\mu})}{\partial\lambda} < 0$ for $k = 1$.

If $k = 2$, using Proposition B.4,

$$
\begin{aligned}
\frac{\partial(1/\overline{\mu})}{\partial\lambda} =& \frac{\partial\left[(1+2\lambda)(\lambda+1) - 2\lambda(\lambda+1)^2\ln\left(\frac{\lambda+1}{\lambda}\right)\right]}{\partial\lambda} \\
\frac{\partial(1/\overline{\mu})}{\partial\lambda} =& (1 + 4\lambda + 2) - 2\left[(\lambda+1)^2 + 2\lambda(\lambda+1)\right]\ln\left(\frac{\lambda+1}{\lambda}\right) - 2\lambda^2(\lambda+1)\left(-\lambda^{-2}\right) \\
\frac{\partial(1/\overline{\mu})}{\partial\lambda} =& (6\lambda + 5) - 2(\lambda+1)(3\lambda+1)\ln\left(\frac{\lambda+1}{\lambda}\right) \\
\frac{\partial(1/\overline{\mu})}{\partial\lambda} =& \lambda^2\left[5\left(\frac{\lambda+1}{\lambda}\right)\left(\frac{1}{\lambda}\right) + \left(\frac{1}{\lambda}\right) - 2\left(\frac{\lambda+1}{\lambda}\right)\left(\frac{\lambda+1}{\lambda} + 2\right)\ln\left(\frac{\lambda+1}{\lambda}\right)\right].
\end{aligned}
$$

Again, let $y \equiv \frac{\lambda+1}{\lambda} \rightarrow \lambda = \frac{1}{y-1}$. However, in this case let $f(y) \equiv 5\left(\frac{\lambda+1}{\lambda}\right)\left(\frac{1}{\lambda}\right) + \left(\frac{1}{\lambda}\right) - 2\left(\frac{\lambda+1}{\lambda}\right)\left(\frac{\lambda+1}{\lambda} + 2\right)\ln\left(\frac{\lambda+1}{\lambda}\right) = 5y(y-1) + (y-1) - 2y(y+2)\ln y \rightarrow f(1) = 0$. As a result, $f'(y) = 10y - 5 + 1 - 2(2y+2)\ln y - 2(y+2) = 8(y-1) - 4(y+1)\ln y \rightarrow f'(1) = 0$, $f''(y) = 8 - 4\ln y - 4\left(\frac{y+1}{y}\right) \rightarrow f''(1) = 0$, and $f'''(y) = -\frac{4}{y} + \frac{4}{y^2} = 4\left(\frac{1-y}{y^2}\right)$. Since $\lambda > 0 \rightarrow y > 1$, $f'''(y) < 0 \xrightarrow{f''(1)=0} f''(y) < 0 \xrightarrow{f'(1)=0} f'(y) < 0 \xrightarrow{f(1)=0} f(y) < 0$, implying $\frac{\partial(1/\overline{\mu})}{\partial\lambda} < 0$ for $k = 2$.

If $k \neq 0, 1, 2$, using again Proposition B.4,

$$
\frac{\partial(1/\overline{\mu})}{\partial\lambda} = \frac{\partial\left[\left(1 + \frac{2\lambda}{2-k}\right) - \frac{k(1-k)/(2-k)}{k - \lambda\left[\left(\frac{\lambda+1}{\lambda}\right)^k - 1\right]}\right]}{\partial\lambda}
$$

$$\frac{\partial(1/\overline{\mu})}{\partial\lambda} = \frac{2}{2-k} + \left[\frac{k(1-k)}{2-k}\right] \frac{-\left[\left(\frac{\lambda+1}{\lambda}\right)^k - 1\right] - \lambda\left[k\left(\frac{\lambda+1}{\lambda}\right)^{k-1}\left(-\frac{1}{\lambda^2}\right)\right]}{\left\{k - \lambda\left[\left(\frac{\lambda+1}{\lambda}\right)^k - 1\right]\right\}^2}$$

$$\frac{\partial(1/\overline{\mu})}{\partial\lambda} = \frac{2}{2-k} + \left[\frac{k(1-k)}{2-k}\right] \frac{\frac{k}{\lambda}\left(\frac{\lambda+1}{\lambda}\right)^{k-1} - \left[\left(\frac{\lambda+1}{\lambda}\right)^k - 1\right]}{\left\{k - \lambda\left[\left(\frac{\lambda+1}{\lambda}\right)^k - 1\right]\right\}^2}$$

$$\frac{\partial(1/\overline{\mu})}{\partial\lambda} = \frac{\frac{2}{2-k}\left\{k - \lambda\left[\left(\frac{\lambda+1}{\lambda}\right)^k - 1\right]\right\}^2 + \frac{k(1-k)}{2-k}\left\{\frac{k}{\lambda}\left(\frac{\lambda+1}{\lambda}\right)^{k-1} - \left[\left(\frac{\lambda+1}{\lambda}\right)^k - 1\right]\right\}}{\left\{k - \lambda\left[\left(\frac{\lambda+1}{\lambda}\right)^k - 1\right]\right\}^2}.$$

Let $k \in (0,2) \setminus \{1\}$, when $2-k > 0$. Assume one more time $y \equiv \frac{\lambda+1}{\lambda} \to \lambda = \frac{1}{y-1}$ and, in this case, let

$$f(y) \equiv 2\left\{k - \lambda\left[\left(\frac{\lambda+1}{\lambda}\right)^k - 1\right]\right\}^2 - k(k-1)\left\{\frac{k}{\lambda}\left(\frac{\lambda+1}{\lambda}\right)^{k-1} - \left[\left(\frac{\lambda+1}{\lambda}\right)^k - 1\right]\right\}$$

$$f(y) = 2\left[k - \left(\frac{y^k-1}{y-1}\right)\right]^2 - k(k-1)\left[k(y-1)y^{k-1} - \left(y^k-1\right)\right] \to \lim_{y\to 1^+} f(y) = 0$$

$$f'(y) = -4\left[k - \left(\frac{y^k-1}{y-1}\right)\right]\left[\frac{ky^{k-1}(y-1) - (y^k-1)}{(y-1)^2}\right] - k(k-1)\left[k^2y^{k-1} - k(k-1)y^{k-2} - ky^{k-1}\right]$$

$$f'(y) = \frac{-4}{y-1}\left[k - \left(\frac{y^k-1}{y-1}\right)\right]\left[k - \left(\frac{y^k-1}{y-1}\right) + k(y^{k-1}-1)\right] - k^2(k-1)^2(y-1)y^{k-2}$$

$$f'(y) = \frac{-1}{y-1}\left\{4\left[k - \left(\frac{y^k-1}{y-1}\right)\right]^2 + 4\left[k - \left(\frac{y^k-1}{y-1}\right)\right]k(y^{k-1}-1) + k^2(k-1)^2(y-1)^2y^{k-2}\right\}$$

$$f'(y) = \frac{-1}{y-1}\left\{\left[2\left(k - \left(\frac{y^k-1}{y-1}\right)\right) + k(y^{k-1}-1)\right]^2 + k^2\left[(k-1)^2(y-1)^2y^{k-2} - (y^{k-1}-1)^2\right]\right\}$$

$$g(y) \equiv (k-1)^2(y-1)^2y^{k-2} - (y^{k-1}-1)^2 \to g(1) = 0$$

$$g'(y) = 2(k-1)^2(y-1)y^{k-2} + (k-1)^2(y-1)^2(k-2)y^{k-3} - 2(y^{k-1}-1)(k-1)y^{k-2}$$

$$h(y) \equiv \frac{g(y)}{y^{k-3}} = 2(k-1)^2(y^2-y) + (k-1)^2(k-2)(y-1)^2 - 2(k-1)(y^k-y) \to h(1) = 0$$

$$h'(y) = 2(k-1)^2(2y-1) + 2(k-1)^2(k-2)(y-1) - 2(k-1)(ky^{k-1}-1) \to h'(1) = 0$$

$$h''(y) = 4(k-1)^2 + 2(k-1)^2(k-2) - 2k(k-1)^2y^{k-2} \to h''(1) = 0$$

$$h'''(y) = -2k(k-1)^2(k-2)y^{k-3} = 2(k-1)^2y^{k-3}k(2-k).$$

Since $\lambda > 0 \to y > 1$ and $k \in (0,2) \setminus \{1\} \to k(2-k) > 0$, $h'''(y) > 0 \xrightarrow{h''(1)=0}$ $h''(y) > 0 \xrightarrow{h'(1)=0} h'(y) > 0 \xrightarrow{h(1)=0} h(y) > 0 \to g'(y) > 0 \xrightarrow{g(1)=0} g(y) > 0 \to f'(y) <$

$0 \xrightarrow{\lim_{y\to 1^+} f(y)=0} f(y) < 0$. Hence, $\frac{\partial(1/\overline{\mu})}{\partial\lambda} < 0$ for $k \in (0,2) \setminus \{1\}$.

In short, $\frac{\partial(1/\overline{\mu})}{\partial\lambda} < 0$ for $k \in (0,2]$. ■

Proposition B.6 *For $k \neq 0$ and $\lambda > 0$, $\lim_{\lambda\to 0^+} \overline{\mu} = \max\{2-k, 1\}$.*

Proof. Let $\lambda > 0$. It is sufficient to show $\lim_{\lambda\to 0^+}(1/\overline{\mu}) = (2-k)^{-1}$ if $k < 1$, $k \neq 0$, and $\lim_{\lambda\to 0^+}(1/\overline{\mu}) = 1$ if $k \geq 1$. If $k = 1$, from Proposition B.4,

$$\lim_{\lambda\to 0^+}(1/\overline{\mu}) = \lim_{\lambda\to 0^+}\left[(1+2\lambda) - \frac{1}{(\lambda+1)\ln\left(\frac{\lambda+1}{\lambda}\right) - 1}\right] = 1 + \frac{1}{1 - \lim_{\lambda\to 0^+}\ln\left(\frac{\lambda+1}{\lambda}\right)} = 1.$$

If $k = 2$, using Proposition B.4,

$$\lim_{\lambda\to 0^+}(1/\overline{\mu}) = \lim_{\lambda\to 0^+}\left[(1+2\lambda)(\lambda+1) - 2\lambda(\lambda+1)^2\ln\left(\frac{\lambda+1}{\lambda}\right)\right] = 1 - 2\lim_{\lambda\to 0^+}\left[\frac{\ln\left(\frac{\lambda+1}{\lambda}\right)}{\lambda^{-1}}\right]$$

$$\lim_{\lambda\to 0^+}(1/\overline{\mu}) = = 1 - 2\lim_{\lambda\to 0^+}\left[\frac{\left(\frac{\lambda}{\lambda+1}\right)(-\lambda^{-2})}{-\lambda^{-2}}\right] = 1 - 0 = 1,$$

where we apply L'Hôpital's rule in the second line.

Lastly, if $k \neq 0, 1, 2$, using again Proposition B.4,

$$\lim_{\lambda\to 0^+}(1/\overline{\mu}) = \lim_{\lambda\to 0^+}\left[\left(1 + \frac{2\lambda}{2-k}\right) - \frac{k(1-k)/(2-k)}{k - \lambda\left[\left(\frac{\lambda+1}{\lambda}\right)^k - 1\right]}\right] = 1 - \frac{k(1-k)/(2-k)}{k - \lim_{\lambda\to 0^+}\left[\frac{\left(\frac{\lambda+1}{\lambda}\right)^k}{\lambda^{-1}}\right]}$$

$$\lim_{\lambda\to 0^+}(1/\overline{\mu}) = \begin{cases} 1 - \frac{k(1-k)}{k(2-k)} = \frac{1}{2-k} & \text{, if } k < 0 \\ 1 - \frac{k(1-k)/(2-k)}{k - \lim_{\lambda\to 0^+}\left[\frac{k\left(\frac{\lambda+1}{\lambda}\right)^{k-1}(-\lambda^{-2})}{-\lambda^{-2}}\right]} = 1 - \frac{k(1-k)}{k(2-k)} = \frac{1}{2-k} & \text{, if } k \in (0,1) \\ 1 - \frac{k(1-k)/(2-k)}{k - \lim_{\lambda\to 0^+}\left[\frac{k\left(\frac{\lambda+1}{\lambda}\right)^{k-1}(-\lambda^{-2})}{-\lambda^{-2}}\right]} = 1 - 0 = 1 & \text{, if } k > 1, k \neq 2 \end{cases},$$

where we use L'Hôpital's rule for $k \in (0,1)$ and $k > 1$, $k \neq 2$. ■

Proposition B.7 *For $k \neq 0$ and $\lambda > 0$, $\lim_{\lambda\to+\infty} \overline{\mu} = 3$.*

Proof. Let $\lambda > 0$. It is sufficient to show $\lim_{\lambda\to+\infty}(1/\overline{\mu}) = 1/3$ for $k \neq 0$. If $k = 1$, from Proposition B.4,

$$\lim_{\lambda\to+\infty}(1/\overline{\mu}) = \lim_{\lambda\to+\infty}\left[1 + \frac{2\lambda(\lambda+1)\ln\left(\frac{\lambda+1}{\lambda}\right) - 2\lambda - 1}{(\lambda+1)\ln\left(\frac{\lambda+1}{\lambda}\right) - 1}\right] = 1 + \lim_{\lambda\to+\infty}\left[\frac{2\ln\left(\frac{\lambda+1}{\lambda}\right) - \frac{2\lambda+1}{\lambda(\lambda+1)}}{\frac{1}{\lambda}\ln\left(\frac{\lambda+1}{\lambda}\right) - \frac{1}{\lambda(\lambda+1)}}\right]$$

$$\lim_{\lambda\to+\infty}(1/\overline{\mu}) = 1 + \lim_{\lambda\to+\infty}\left[\frac{2\left(\frac{\lambda}{\lambda+1}\right)\left(-\frac{1}{\lambda^2}\right) - \frac{2\lambda(\lambda+1)-(2\lambda+1)(2\lambda+1)}{\lambda^2(\lambda+1)^2}}{-\frac{1}{\lambda^2}\ln\left(\frac{\lambda+1}{\lambda}\right) + \frac{1}{\lambda}\left(\frac{\lambda}{\lambda+1}\right)\left(-\frac{1}{\lambda^2}\right) + \frac{2\lambda+1}{\lambda^2(\lambda+1)^2}}\right]$$

$$\lim_{\lambda\to+\infty}(1/\overline{\mu}) = 1 + \lim_{\lambda\to+\infty}\left[\frac{-\frac{2\lambda}{\lambda+1} - \frac{2\lambda}{\lambda+1} + \left(\frac{2\lambda+1}{\lambda+1}\right)^2}{-\ln\left(\frac{\lambda+1}{\lambda}\right) - \frac{\lambda+1}{(\lambda+1)^2} + \frac{2\lambda+1}{(\lambda+1)^2}}\right] = 1 + \lim_{\lambda\to+\infty}\left[\frac{\left(\frac{2\lambda+1}{\lambda+1}\right)^2 - \frac{4\lambda}{\lambda+1}}{\frac{\lambda}{(\lambda+1)^2} - \ln\left(\frac{\lambda+1}{\lambda}\right)}\right]$$

$$\lim_{\lambda\to+\infty}(1/\overline{\mu}) = 1 + \lim_{\lambda\to+\infty}\left[\frac{2\left(\frac{2\lambda+1}{\lambda+1}\right)\left(\frac{2(\lambda+1)-(2\lambda+1)}{(\lambda+1)^2}\right) - \frac{4(\lambda+1)-4\lambda}{(\lambda+1)^2}}{\frac{(\lambda+1)^2-2\lambda(\lambda+1)}{(\lambda+1)^4} - \left(\frac{\lambda}{\lambda+1}\right)\left(-\frac{1}{\lambda^2}\right)}\right]$$

$$\lim_{\lambda\to+\infty}(1/\overline{\mu}) = 1 + \lim_{\lambda\to+\infty}\left[\frac{2\left(\frac{2\lambda+1}{\lambda+1}\right) - 4}{\frac{\lambda+1}{\lambda} - \frac{\lambda-1}{\lambda+1}}\right] = 1 + \lim_{\lambda\to+\infty}\left[\frac{2\left(\frac{2(\lambda+1)-(2\lambda+1)}{(\lambda+1)^2}\right)}{-\frac{1}{\lambda^2} - \frac{(\lambda+1)-(\lambda-1)}{(\lambda+1)^2}}\right]$$

$$\lim_{\lambda\to+\infty}(1/\overline{\mu}) = 1 + \lim_{\lambda\to+\infty}\left[\frac{\frac{2}{(\lambda+1)^2}}{-\frac{1}{\lambda^2} - \frac{2}{(\lambda+1)^2}}\right] = 1 - \lim_{\lambda\to+\infty}\left[\frac{2}{\left(\frac{\lambda+1}{\lambda}\right)^2 + 2}\right] = 1 - \frac{2}{1+2} = \frac{1}{3},$$

where we apply L'Hôpital's rule in the second, fourth, and fifth lines.

If $k = 2$, using Proposition B.4,

$$\lim_{\lambda\to+\infty}(1/\overline{\mu}) = \lim_{\lambda\to+\infty}\left[\frac{\frac{1+2\lambda}{\lambda(\lambda+1)} - 2\ln\left(\frac{\lambda+1}{\lambda}\right)}{\lambda^{-1}(\lambda+1)^{-2}}\right] = \lim_{\lambda\to+\infty}\left[\frac{\frac{2\lambda(\lambda+1)-(2\lambda+1)(2\lambda+1)}{\lambda^2(\lambda+1)^2} - 2\left(\frac{\lambda}{\lambda+1}\right)\left(-\frac{1}{\lambda^2}\right)}{-\lambda^{-2}(\lambda+1)^{-2} - 2\lambda^{-1}(\lambda+1)^{-3}}\right]$$

$$\lim_{\lambda\to+\infty}(1/\overline{\mu}) = \lim_{\lambda\to+\infty}\left[\frac{2\lambda(\lambda+1) - (2\lambda+1)(\lambda+\lambda+1) + 2\lambda(\lambda+1)}{-1 - \frac{2\lambda}{\lambda+1}}\right]$$

$$\lim_{\lambda\to+\infty}(1/\overline{\mu}) = \lim_{\lambda\to+\infty}\left[\frac{4\lambda(\lambda+1) - 2\lambda^2 - 2\lambda(\lambda+1) - (2\lambda+1)}{-1 - \frac{2\lambda}{\lambda+1}}\right]$$

$$\lim_{\lambda\to+\infty}(1/\overline{\mu}) = \lim_{\lambda\to+\infty}\left[\frac{2\lambda(\lambda+1) - 2\lambda^2 - (2\lambda+1)}{-1 - \frac{2\lambda}{\lambda+1}}\right] = \lim_{\lambda\to+\infty}\left[\frac{1}{1 + \frac{2\lambda}{\lambda+1}}\right] = \frac{1}{1+2} = \frac{1}{3},$$

where we apply L'Hôpital's rule in the first line.

Finally, If $k \neq 0, 1, 2$, using again Proposition B.4,

$$\lim_{\lambda\to+\infty}(1/\overline{\mu}) = \lim_{\lambda\to+\infty}\left[1 + \left(\frac{1}{2-k}\right)\frac{\frac{2k}{\lambda} - 2\left[\left(\frac{\lambda+1}{\lambda}\right)^k - 1\right] - \frac{k(1-k)}{\lambda^2}}{\frac{k}{\lambda^2} - \frac{1}{\lambda}\left[\left(\frac{\lambda+1}{\lambda}\right)^k - 1\right]}\right]$$

$$\lim_{\lambda\to+\infty}(1/\overline{\mu}) = 1 + \left(\frac{1}{2-k}\right)\lim_{\lambda\to+\infty}\left[\frac{-\frac{2k}{\lambda^2} - 2k\left(\frac{\lambda+1}{\lambda}\right)^{k-1}\left(-\frac{1}{\lambda^2}\right) + 2\frac{k(1-k)}{\lambda^3}}{-2\frac{k}{\lambda^3} + \frac{1}{\lambda^2}\left[\left(\frac{\lambda+1}{\lambda}\right)^k - 1\right] - \frac{1}{\lambda}k\left(\frac{\lambda+1}{\lambda}\right)^{k-1}\left(-\frac{1}{\lambda^2}\right)}\right]$$

$$\lim_{\lambda\to+\infty}(1/\overline{\mu}) = 1 + \left(\frac{2k}{2-k}\right)\lim_{\lambda\to+\infty}\left[\frac{\left(\frac{\lambda+1}{\lambda}\right)^{k-1} - 1 + \frac{(1-k)}{\lambda}}{\left(\frac{\lambda+1}{\lambda}\right)^k - 1 + \frac{k}{\lambda}\left[\left(\frac{\lambda+1}{\lambda}\right)^{k-1} - 2\right]}\right]$$

$$\lim_{\lambda\to+\infty}(1/\overline{\mu}) = 1 + \left(\frac{2k}{2-k}\right)\lim_{\lambda\to+\infty}\left[\frac{-(k-1)\left(\frac{\lambda+1}{\lambda}\right)^{k-2} - (1-k)}{-k\left(\frac{\lambda+1}{\lambda}\right)^{k-1} - k\left[\left(\frac{\lambda+1}{\lambda}\right)^{k-1} - 2\right] - \frac{k}{\lambda}(k-1)\left(\frac{\lambda+1}{\lambda}\right)^{k-2}}\right]$$

$$\lim_{\lambda\to+\infty}(1/\overline{\mu}) = 1 + \left[\frac{2k(1-k)}{2-k}\right]\lim_{\lambda\to+\infty}\left[\frac{\left(\frac{\lambda+1}{\lambda}\right)^{k-2}-1}{-2k\left[\left(\frac{\lambda+1}{\lambda}\right)^{k-1}-1\right]-\frac{k}{\lambda}(k-1)\left(\frac{\lambda+1}{\lambda}\right)^{k-2}}\right]$$

$$\lim_{\lambda\to+\infty}(1/\overline{\mu}) = 1 + \lim_{\lambda\to+\infty}\left[\frac{2k(1-k)\left(\frac{\lambda+1}{\lambda}\right)^{k-3}}{2k(k-1)\left(\frac{\lambda+1}{\lambda}\right)^{k-2}+k(k-1)\left(\frac{\lambda+1}{\lambda}\right)^{k-2}+\frac{k}{\lambda}(k-1)(k-2)\left(\frac{\lambda+1}{\lambda}\right)^{k-3}}\right]$$

$$\lim_{\lambda\to+\infty}(1/\overline{\mu}) = 1 + \frac{2k(1-k)}{2k(k-1)+k(k-1)} = 1 - \frac{2k(k-1)}{3k(k-1)} = 1 - \frac{2}{3} = \frac{1}{3},$$

where we apply L'Hôpital's rule in the second, fourth, and sixth lines. ■

Proposition B.8 *For $k \in (0,2]$ and $\lambda > 0$, $\tilde{A} \equiv \overline{A}/\underline{A}$, $\tilde{A} > 1$, is a continuous, strictly increasing, and well-defined function of μ if and only if $\mu \in (1,3)$ and $\lambda > \lambda^*(\mu)$, where $\lambda^*(\mu) \equiv \arg\min_{x\in[0,+\infty]} \lim_{\lambda\to x} |\overline{\mu} - \mu|$.*

Proof. Let $\hat{g}_s$ be the density of a truncated Lomax distribution with shape parameter $k \in (0,2]$ and scale parameter $\lambda > 0$ defined over $\tilde{s}(A) \in [0, \tilde{s}(A_h)]$, $A_h > \overline{A} > \underline{A}$, with $\hat{G}_s$ being the respective cumulative distribution function. It is easy to see $\tilde{g}_s(\tilde{s}(A)) = \hat{g}_s(\tilde{s}(A))/\hat{G}_s(\tilde{s}(\overline{A}))$ is the density of a truncated Lomax distribution with the same parameters $k \in (0,2]$ and $\lambda > 0$ over the support $[0, \tilde{s}(\overline{A})]$.[23] Given the density $\tilde{g}_s$ ($\hat{g}_s$), one gets the respective density for $A \in \left[\underline{A}, \overline{A}\right]$ ($A \in [\underline{A}, A_h]$), which we denote by $\tilde{g}$ ($\hat{g}$), with cumulative distribution function $\tilde{G}$ ($\hat{G}$). To get these distributions, note that, for any $A^* \in [\underline{A}, \overline{A}]$,

$$P(A < A^*) = P(\underline{A}/A^* < \underline{A}/A) = P(1 - \underline{A}/A < 1 - \underline{A}/A^*) = P(\tilde{s}(A) < \tilde{s}(A^*)),$$

implying $\tilde{G}(A) = \tilde{G}_s(\tilde{s}(A)) \to \tilde{g}(A) = \tilde{g}_s(\tilde{s}(A))\underline{A}/A^2$ and $\hat{G}(A) = \hat{G}_s(\tilde{s}(A)) \to \hat{g}(A) = \hat{g}_s(\tilde{s}(A))\underline{A}/A^2$. Given these distributions and since $\tilde{g}_s(\tilde{s}(A)) = \hat{g}_s(\tilde{s}(A))/\hat{G}_s(\tilde{s}(\overline{A}))$,

$$\frac{\hat{g}(A)}{\hat{G}(\overline{A})} = \left[\frac{\hat{g}_s(\tilde{s}(A))}{\hat{G}_s(\tilde{s}(\overline{A}))}\right]\underline{A}/A^2 = \tilde{g}_s(\tilde{s}(A))\underline{A}/A^2 = \tilde{g}(A),$$

which allows us to use Proposition B.1. Thus, $\overline{A}$, $\overline{A} > \underline{A}$ is continuous, strictly increasing, and well defined in μ if and only if $\mu \in (1, \overline{\mu})$, where $\overline{\mu}$ is given in Proposition B.4. Since μ is only a function of $\tilde{A} \equiv \overline{A}/\underline{A}$ (given k and λ) due to Proposition B.3 and the fact that $S \equiv \frac{\tilde{s}(\overline{A})}{\lambda} + 1 = \frac{1-\tilde{A}^{-1}}{\lambda} + 1$, these features of $\overline{A}$ also hold for $\tilde{A}$.

From Propositions B.5, B.6, and B.7, the image of $\overline{\mu}$ over $\lambda \in (0, +\infty)$ is $(\max\{2-k, 1\}, 3)$ for $k \in (0,2]$. Hence, any $k \in (0,2]$ is viable in the sense that there is always $\lambda > 0$ such as $\mu \in (1, \overline{\mu})$ if and only if $\mu \in (1,3)$. Under such condition, from Proposition B.5, any $\lambda > \lambda^*(\mu)$ is viable, where $\lambda^*(\mu) \equiv \arg\min_{x\in[0,+\infty]} \lim_{\lambda\to x} |\overline{\mu} - \mu|$ for $k \in (0,2]$, which is well defined

[23] After all, the Lomax density is the density of a Pareto with the support shifted by $\lambda > 0$.

as $\overline{\mu}$ is a continuous and monotonic function of λ (Proposition B.5).[24] Therefore, for $k \in (0, 2]$ and $\lambda > 0$, $\mu \in (1, \overline{\mu})$ holds if and only if $\mu \in (1, 3)$ and $\lambda > \lambda^*(\mu)$. ■

Figure B.1 illustrates the results of Proposition B.8, plotting $\tilde{A}$ against μ for truncated Lomax distributions with $k = 1$ and $\lambda = 10, 1, 0.1, 0.01$.

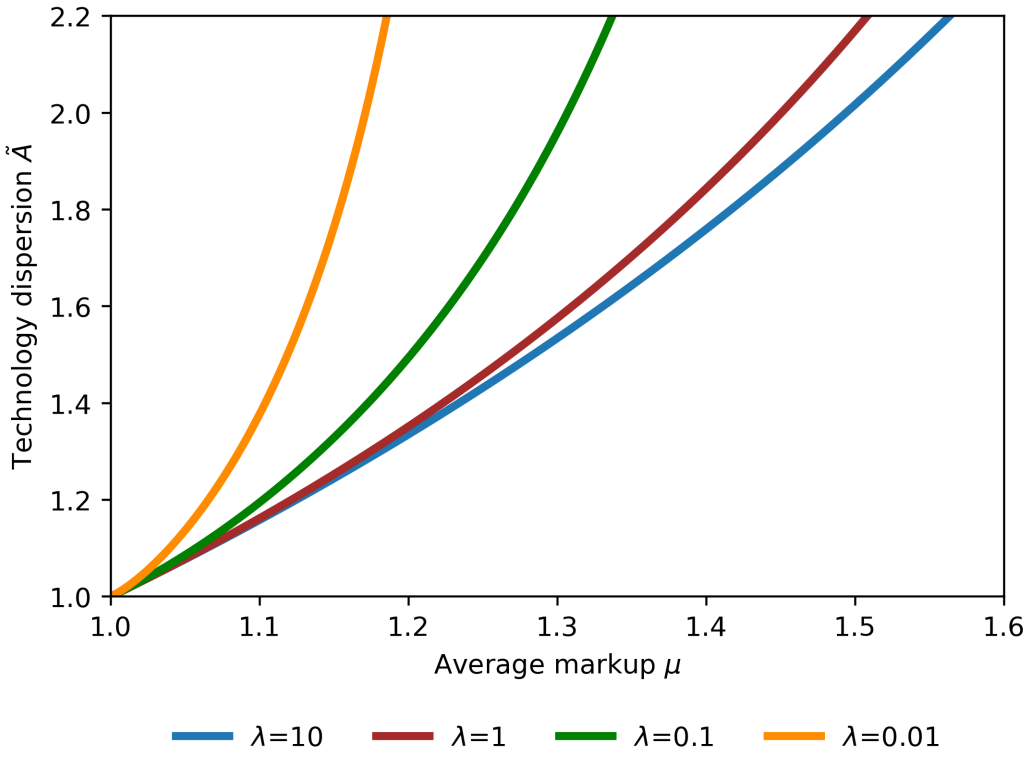

Figure B.1: Technological dispersion $\tilde{A} \equiv \overline{A}/\underline{A}$ *versus* average markup μ – Zipf's law calibration with $k = 1$.

We finish this section with a comment about the generalization of Propositions B.5 and B.8 for any $k \neq 0$. In Proposition B.5, we show

$$\frac{\partial(1/\overline{\mu})}{\partial\lambda} = \frac{2}{2-k} + \left[\frac{k(1-k)}{2-k}\right] \frac{\frac{k}{\lambda}\left(\frac{\lambda+1}{\lambda}\right)^{k-1} - \left[\left(\frac{\lambda+1}{\lambda}\right)^{k} - 1\right]}{\left\{k - \lambda\left[\left(\frac{\lambda+1}{\lambda}\right)^{k} - 1\right]\right\}^2}$$

for any $k \neq 0, 1, 2$. Consequently, if $k = -1$,

$$\frac{\partial(1/\overline{\mu})}{\partial\lambda} = \frac{2}{3}\left\{1 - \frac{-\frac{1}{\lambda}\left(\frac{\lambda}{\lambda+1}\right)^2 - \left(\frac{\lambda}{\lambda+1}\right) + 1}{\left[-1 - \lambda\left(\frac{\lambda}{\lambda+1}\right) + \lambda\right]^2}\right\} = \frac{2}{3}\left\{1 - \frac{\frac{1}{\lambda+1}\left[(\lambda+1) - \lambda - \left(\frac{\lambda}{\lambda+1}\right)\right]}{\left[(\lambda-1) - \frac{\lambda^2}{\lambda+1}\right]^2}\right\}$$

$$\frac{\partial(1/\overline{\mu})}{\partial\lambda} = \frac{2}{3}\left\{1 - \frac{\frac{1}{\lambda+1}\left[\frac{(\lambda+1)-\lambda}{\lambda+1}\right]}{\left[\frac{(\lambda-1)(\lambda+1)-\lambda^2}{\lambda+1}\right]^2}\right\} = \frac{2}{3}\left\{1 - \frac{\frac{1}{\lambda+1}\left(\frac{1}{\lambda+1}\right)}{\left(\frac{-1}{\lambda+1}\right)^2}\right\} = \frac{2}{3}(1-1) = 0.$$

[24] Note $\overline{\mu} = \mu$ under $\lambda = \lambda^*(\mu) \in (0, +\infty)$ except for $k \in (0, 1)$ and $\mu \in (1, 2-k]$, when $\lambda^*(\mu) = 0$ as $\overline{\mu}$ is strictly increasing in $\lambda > 0$ with $\overline{\mu} \in (2-k, 3)$.

Moreover, numerical results using this expression, such as those shown in Figure B.2, suggest $\frac{\partial(1/\overline{\mu})}{\partial\lambda} > 0$ for $k < -1$ and $\frac{\partial(1/\overline{\mu})}{\partial\lambda} < 0$ for $k \in (-1, 0) \cup (2, +\infty)$. Assuming these results indeed hold, one can generalize Proposition B.5 for any $k \neq 0$: for $\lambda > 0$, $\frac{\partial\overline{\mu}}{\partial\lambda} > 0$ if $k > -1, k \neq 0$, $\frac{\partial\overline{\mu}}{\partial\lambda} = 0$ if $k = -1$, and $\frac{\partial\overline{\mu}}{\partial\lambda} < 0$ if $k < -1$.

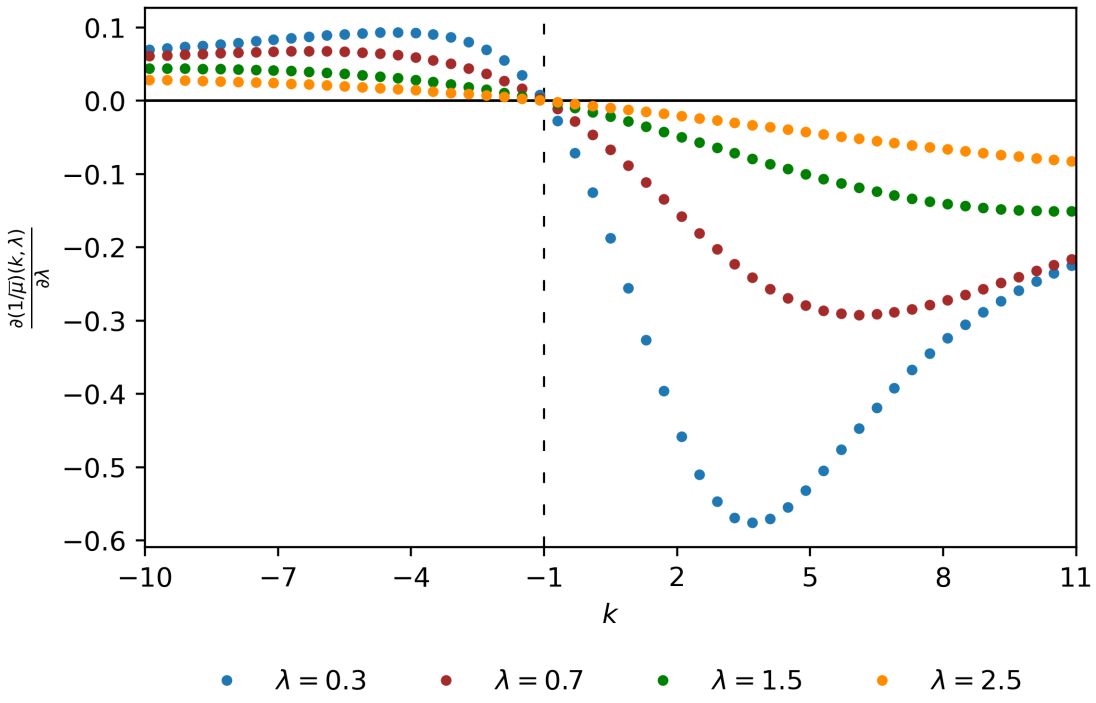

Figure B.2: $\frac{\partial(1/\overline{\mu})}{\partial\lambda}$ *versus* k, $k \neq 0, 1, 2$.

Given this (possible) new Proposition B.5, one can also generalize Proposition B.8: for $k \neq 0$ and $\lambda > 0$, $\tilde{A} \equiv \overline{A}/\underline{A}$, $\tilde{A} > 1$, is continuous, strictly increasing, and well defined in μ if and only if (i) $\mu \in (1, 3)$, (ii) $\mu = 3$ and $k \leq -1$, or (iii) $\mu > 3$ and $k < 2 - \mu < -1$, with any viable λ, that is, with

$$\lambda \in \begin{cases} (0, \lambda^*(\mu)) & \text{, if } k < -1 \\ (0, +\infty) & \text{, if } k = -1 \\ (\lambda^*(\mu), +\infty) & \text{, if } k > -1, k \neq 0 \end{cases},$$

where $\lambda^*(\mu) \equiv \arg\min_{x \in [0,+\infty]} \lim_{\lambda \to x} |\overline{\mu} - \mu|$ is now defined for any $k \notin \{-1, 0\}$.[25] After all, in this case, from this (possible) new Proposition B.5 and Propositions B.6 and B.7, the image

[25]Here, given this (possible) new Proposition B.5, $\overline{\mu} = \mu$ under $\lambda^*(\mu) \in (0, +\infty)$ except in two cases. The first exception would be $k < -1$ and $\mu \in (1, 3]$, when $\lambda^*(\mu) = +\infty$ as $\overline{\mu}$ is strictly decreasing in $\lambda > 0$ with $\overline{\mu} \in (3, 2 - k)$. The second exception would be $k \in (-1, 1) \setminus \{0\}$ and $\mu \in (1, 2 - k]$, when $\lambda^* = 0$ as $\overline{\mu}$ is strictly increasing in $\lambda > 0$ with $\overline{\mu} \in (2 - k, 3)$.

of $\overline{\mu}$ over $\lambda \in (0, +\infty)$ is

$$\begin{cases} (3, 2-k) & \text{, if } k < -1 \\ [3,3] & \text{, if } k = -1 \\ (\max\{2-k, 1\}, 3) & \text{, if } k > -1, k \neq 0 \end{cases},$$

implying any $k \neq 0$ is viable if $\mu \in (1,3)$; if $\mu = 3$, $k \leq -1$; if $\mu > 3$, $\mu < 2 - k \rightarrow k < 2 - \mu < -1$. And, given a viable k, from this (possible) generalization of Proposition B.5, one easily gets the viable λs shown in the statement of the (possible) new Proposition B.8.

C Zipf's law calibration

In this section, we outline the calibration strategy for the case where firm market share follows a truncated Lomax distribution. We begin by discussing this alternative distributional assumption and its relationship with Zipf's law. Finally, we present the two-stage calibration procedure, which is similar to the one discussed in Section 3.3 for the baseline model. We do not elaborate on the computation of the target moments using real-world data, as it can be done in the same way as before (see Section 3.2 for details).

C.1 Distributional assumption and Zipf's law

Suppose $\tilde{s}(A) \equiv 1 - \underline{A}/A = \frac{s(A)}{\eta/q} \in \left[0, \tilde{s}(\overline{A})\right] = \left[0, 1 - \tilde{A}^{-1}\right]$ is truncated Lomax distributed with shape parameter $k \neq 0$ and scale parameter $\lambda > 0$, or equivalently, $(\tilde{s}(A)+\lambda) \in [\lambda, \tilde{s}(\overline{A})+\lambda]$ is truncated Pareto distributed with shape parameter $k \neq 0$. Thus, the density of $\tilde{s}(A)$ is $\tilde{g}_s(\tilde{s}(A)) = k \left[\frac{\lambda^k (\tilde{s}(\overline{A})+\lambda)^k}{(\tilde{s}(\overline{A})+\lambda)^k - \lambda^k}\right] (\tilde{s}(A) + \lambda)^{-k-1}$, which is shown in Figure C.1 for $k = 1$ and $\lambda = 0.2, 0.4, 1$, with $\tilde{s}(\overline{A}) = 1/3$.[26]

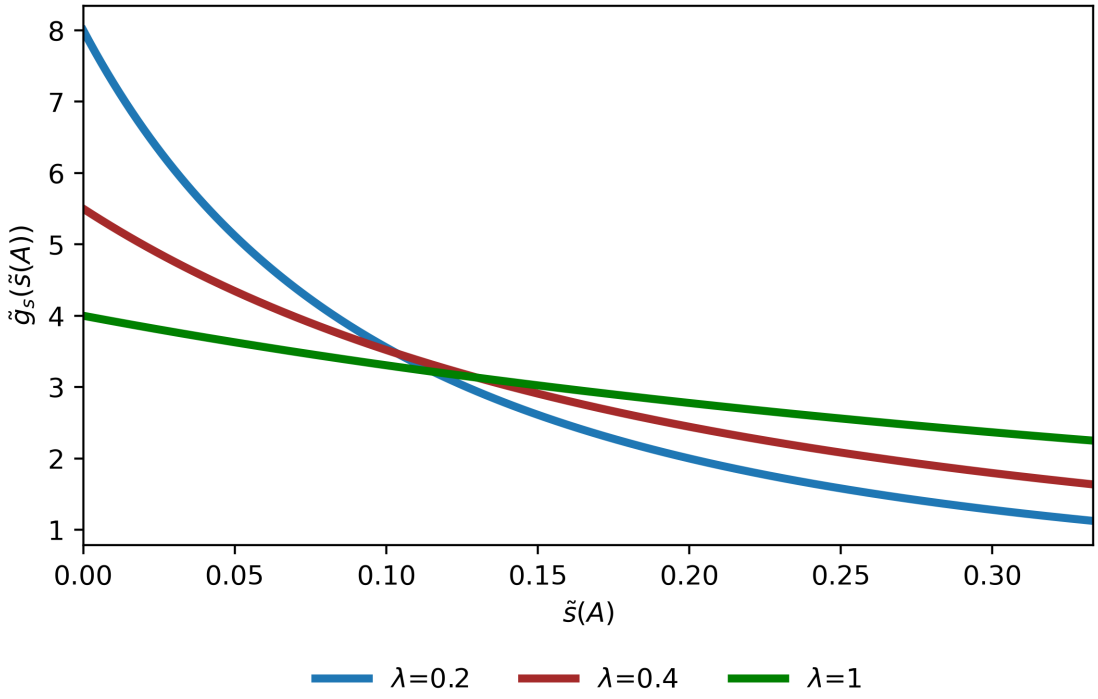

Figure C.1: Truncated Lomax density with $k = 1$ and support $[0, 1/3]$.

For $k \approx 1$ and $\lambda \approx 0$, firm market share is approximately truncated Pareto distributed with

[26] Alternatively, we could have imposed the distribution of $\theta_i = L_i/L = K_i/K$, when firm size would be measured by number of employees (or capital stock) instead of sales. Since we need $\mathrm{E}_a\left[(\underline{A}/A)^j\right]$ for $j \in \mathbb{N} \setminus \{0\}$ to compute the target moments, we should recover $\underline{A}/A_i$ from θ_i. Given Equation (2) for the continuous model and (A.1), $\theta_i = \frac{\overline{A}\Omega}{\underline{A}} (\eta/q) \left[(\underline{A}/A_i) - (\underline{A}/A_i)^2\right]$ and thus θ_i uniquely identifies $\underline{A}/A_i$ if and only if $\tilde{A} \equiv \overline{A}/\underline{A} \leq 2$. Thus, under this alternative strategy, one must impose $\tilde{A} \leq 2$, which may not hold empirically.

shape parameter $k \approx 1$, consistent with Zipf's law, particularly away from the bounds of the support. After all,

$$P\left(\tilde{s}(A) \geq x\right) = \int_{x}^{\tilde{s}(\overline{A})} \tilde{g}_s(y)dy = \frac{(x+\lambda)^{-k} - (\tilde{s}(\overline{A})+\lambda)^{-k}}{\lambda^{-k} - (\tilde{s}(\overline{A})+\lambda)^{-k}} \tag{C.1}$$

$$\frac{\partial \ln P\left(\tilde{s}(A) \geq x\right)}{\partial \ln x} = \frac{-k(x+\lambda)^{-k-1}x}{(x+\lambda)^{-k} - (\tilde{s}(\overline{A})+\lambda)^{-k}} = -k\left[\frac{\frac{x}{x+\lambda}}{1-\left(\frac{x+\lambda}{\tilde{s}(\overline{A})+\lambda}\right)^{k}}\right], \tag{C.2}$$

where we use in the last line $\frac{\partial x}{\partial \ln x} = \frac{\partial e^{\ln x}}{\partial \ln x} = e^{\ln x} = x$.[27] As a result, (i) $\frac{\partial \ln P(\tilde{s}(A)\geq x)}{\partial \ln x} \to 0$ as $x \to 0^{+}$, (ii) $\frac{\partial \ln P(\tilde{s}(A)\geq x)}{\partial \ln x} \to -\infty$ as $x \to \tilde{s}(\overline{A})^{-}$, and (iii) $\frac{\partial \ln P(\tilde{s}(A)\geq x)}{\partial \ln x} \approx -k\left(\frac{x}{x+\lambda}\right)$ near the beginning of the support, when $\frac{x+\lambda}{\tilde{s}(\overline{A})+\lambda} \approx 0$. Consequently, if $k \approx 1$ and $\lambda \approx 0$, $\frac{\partial \ln P(\tilde{s}(A)\geq x)}{\partial \ln x} \approx -1$ for x near the beginning of the support, as in Zipf's law.

It is worth mentioning these deviations from Zipf's law near the bounds of the support are not a shortcoming of the Lomax distribution. It would occur for any continuous truncated distribution. On the one hand, there is no distribution satisfying Zipf's law at $x = 0$, since $P(s \geq x) = cx^{-k}$ with $k \approx 1$ is only well defined for $x \neq 0$, implying $\frac{\partial \ln P(\tilde{s}(A)\geq x)}{\partial \ln x}$ should deviate from -1 sufficiently close to $x = 0$ as $P\left(\tilde{s}(A) \geq x\right)$ is a continuous function. On the other hand, to evaluate the behavior near the end of the support, assume, by contradiction, $P(s \geq x) = cx^{-k}$ for $s \in [\underline{s}, \overline{s}] \in (0, +\infty)$ and $k \approx 1$, with $c > 0$ as $P(s \geq x) > 0$ at least for $x = \underline{s}$. In this case, $P(s \geq \overline{s}) = c\overline{s}^{-k} > 0$, which is absurd as $s \in [\underline{s}, \overline{s}] \in (0, +\infty)$ and thus $P(s \geq \overline{s}) = 0$. Therefore, no truncated continuous distribution satisfies Zipf's law over a strictly positive support. A corollary of this result is that any distribution should deviate from Zipf's law near the end of its positive support. After all, if that were not true, by truncating this distribution from below, we would obtain a truncated continuous distribution over a narrow strictly positive support that satisfies Zipf's law, contradicting the previous result.

Under this distributional assumption, we demonstrated in Proposition B.2 that

$$\mathrm{E}_a\left[(\tilde{s}(A)+\lambda)^{j}\right] = \begin{cases} \frac{k\lambda^{j}}{j-k}\left(\frac{S^{j}-S^{k}}{S^{k}-1}\right) & \text{, if } j \neq k \\ k\lambda^{k}\left(\frac{S^{k}\ln S}{S^{k}-1}\right) & \text{, if } j = k \end{cases} \tag{C.3}$$

for $k \neq 0$, $\lambda > 0$, and $j \in \mathbb{N} \setminus \{0\}$, where $S \equiv \frac{\tilde{s}(\overline{A})}{\lambda} + 1$.

C.2 Two-stage calibration procedure

We essentially follow the same two-stage procedure presented in Section 3.3 to quantify the model, but use (C.3) and the fact that $\tilde{s}(A) \equiv 1 - \underline{A}/A \to \mathrm{E}_a\left((\underline{A}/A)^{j}\right) = \mathrm{E}_a\left((1-\tilde{s}(A))^{j}\right)$,

[27] From (C.1), $P\left(s(A) \geq x\right) = P\left(\tilde{s}(A) \geq \frac{x}{\eta/q}\right) = \frac{(x+\tilde{\lambda})^{-k} - (s(\overline{A})+\tilde{\lambda})^{-k}}{\tilde{\lambda}^{-k} - (s(\overline{A})+\tilde{\lambda})^{-k}}$ for $\tilde{\lambda} \equiv \lambda\left(\eta/q\right)$, meaning $s(A) \in [0, s(\overline{A})]$ is truncated Lomax distributed with shape parameter $k \neq 0$ and scale parameter $\tilde{\lambda} > 0$.

instead of Equation (9). In the first stage, we find $\underline{A}$ and $\overline{A}$ by matching aggregate TFP $\overline{A}\Omega$ and average markup μ. From Proposition B.8, given $k \in (0, 2]$, a unique solution to this problem exists if and only if $\mu \in (1, 3)$ and $\lambda > \lambda^*(\mu)$, where $\lambda^*(\mu) \equiv \arg\min_{x \in [0,+\infty]} \lim_{\lambda \to x} |\overline{\mu} - \mu|$ and $\overline{\mu} \equiv \lim_{\overline{A} \to +\infty} \mu$ is computed from (10) in Proposition B.4. Analogous to the baseline Pareto case, for a given distributional shape, allocative efficiency Ω is only a function of μ. Figure C.2 plots this function for truncated Lomax distributions with $k = 1$ and $\lambda = 10, 1, 0.1, 0.01$, showing several noteworthy results. First, as in the baseline case, Ω is strictly decreasing in $\mu = \frac{1-\alpha}{LS}$, with $\Omega \to 1^-$ as $\mu \to 1^+$. Second, given a time series of μ, a higher λ results in a higher and less volatile estimated Ω.

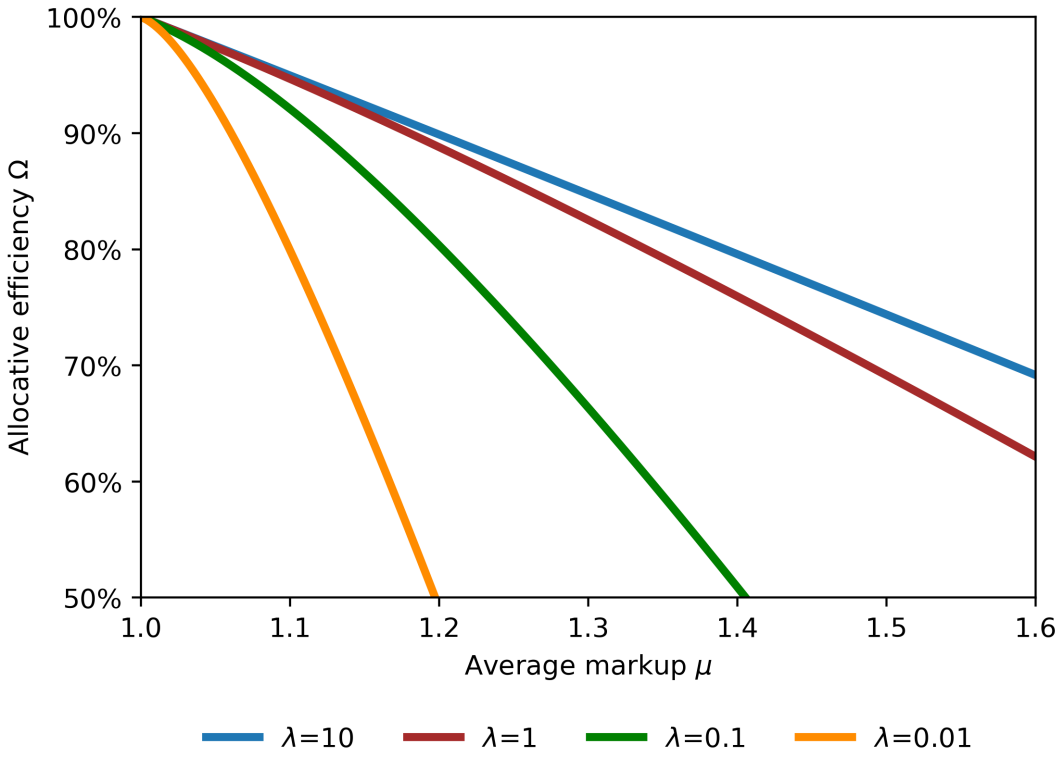

Figure C.2: Allocative efficiency Ω *versus* average markup μ – Zipf's law calibration with $k = 1$.

In the second stage, we set $k \in (0, 2]$, $k \approx 1$, which is viable as $\mu \in (1, 3)$ in Brazil, and search for a time-invariant λ that minimizes the distance to the normalized $N_a HHI_L$.[28] We limit the search to $\lambda > \lambda^*(\max\{\mu\})$, where $\max\{\mu\}$ is the maximum μ in its time series.[29] Analogous to the baseline Pareto case, TFP data are not required to estimate Ω, not even indirectly through λ. They are used solely to pin down $\underline{A}$ and $\overline{A}$. Therefore, once again, the residual from the production function is not the TFP $\overline{A}\Omega$ itself, but only its technology component $\overline{A}$.

[28] We also jointly estimate $k \neq 0$ and $\lambda > 0$ in the second stage. Since $k \in (0, 2]$ may not hold in this case, we rely on a (possible) generalization of Proposition B.8 to any $k \neq 0$ discussed at the end of Appendix B.2.

[29] Given $\mu \in (1, 3)$ and $k \in (0, 2]$, there is a solution for the first-stage algorithm if and only if $\lambda > \lambda^*(\mu)$. As a result, $\lambda > \max\{\lambda^*(\mu)\}$ ensures there is a solution for this algorithm in each period, with $\max\{\lambda^*(\mu)\}$ being the maximum $\lambda^*(\mu)$ in its time series. However, since $\overline{\mu}$ is strictly increasing in λ for $k \in (0, 2]$ (Proposition B.5), $\max\{\lambda^*(\mu)\} = \lambda^*(\max\{\mu\})$.

References

Ackerberg, D. A., K. Caves, and G. Frazer (2015). Identification properties of recent production function estimators. *Econometrica 83*(6), 2411–2451.

Atkeson, A. and A. Burstein (2008). Pricing-to-market, trade costs, and international relative prices. *American Economic Review 98*(5), 1998–2031.

Autor, D., D. Dorn, L. F. Katz, C. Patterson, and J. Van Reenen (2020). The fall of the labor share and the rise of superstar firms. *The Quarterly Journal of Economics 135*(2), 645–709.

Axtell, R. L. (2001). Zipf distribution of U.S. firm sizes. *Science 293*(5536), 1818–1820.

Baqaee, D. R. and E. Farhi (2020). Productivity and misallocation in general equilibrium. *The Quarterly Journal of Economics 135*(1), 105–163.

Barkai, S. (2020). Declining labor and capital shares. *The Journal of Finance 75*(5), 2421–2463.

Basu, S., J. Fernald, J. Fisher, and M. Kimball (2013). Sector-specific technical change. *Manuscript, Federal Reserve Bank of San Francisco*.

Basu, S. and J. G. Fernald (2002). Aggregate productivity and aggregate technology. *European Economic Review 46*(6), 963–991.

Basu, S., J. G. Fernald, and M. S. Kimball (2006). Are technology improvements contractionary? *American Economic Review 96*(5), 1418–1448.

Benkard, C. L., A. Yurukoglu, and A. L. Zhang (2021). Concentration in product markets. *NBER Working Paper Series* (28745).

Bergeaud, A., G. Cette, and R. Lecat (2018). The role of production factor quality and technology diffusion in twentieth-century productivity growth. *Cliometrica 12*(1), 61–97.

Bernard, A. B., J. Eaton, J. B. Jensen, and S. Kortum (2003). Plants and productivity in international trade. *American Economic Review 93*(4), 1268–1290.

Berry, S., M. Gaynor, and F. Scott Morton (2019). Do increasing markups matter? lessons from empirical industrial organization. *Journal of Economic Perspectives 33*(3), 44–68.

Blundell, R. and S. Bond (2000). Gmm estimation with persistent panel data: an application to production functions. *Econometric reviews 19*(3), 321–340.

Busso, M., L. Madrigal, and C. Pagés (2013). Productivity and resource misallocation in Latin America. *The BE Journal of Macroeconomics 13*(1), 903–932.

Calice, P., E. P. Ribeiro, and S. Byskov (2018). Efficient financial allocation and productivity growth in Brazil. *World Bank Policy Research Working Paper* (8479).

Calligaris, S., C. Criscuolo, and L. Marcolin (2018). Mark-ups in the digital era. *OECD Science, Technology and Industry Working Papers* (2018/10).

Carvalho, A. and T. T. O. Santos (2020). Is the equity risk premium compressed in Brazil? *Central Bank of Brazil Working Paper Series* (527).

Comin, D. A., J. Quintana, T. G. Schmitz, and A. Trigari (2023). Revisiting productivity dynamics in Europe: A new measure of utilization-adjusted TFP growth. *NBER Working Paper Series* (31006).

Crafts, N. and P. Woltjer (2021). Growth accounting in economic history: findings, lessons and new directions. *Journal of Economic Surveys 35*(3), 670–696.

Da Silva, S., R. Matsushita, R. Giglio, and G. Massena (2018). Granularity of the top 1,000 Brazilian companies. *Physica A: Statistical Mechanics and its Applications 512*, 68–73.

De Loecker, J. and J. Eeckhout (2018). Global market power. *NBER Working Paper Series* (24768).

De Loecker, J., J. Eeckhout, and S. Mongey (2021). Quantifying market power and business dynamism in the macroeconomy. *NBER Working Paper Series* (28761).

De Vries, G. J. (2014). Productivity in a distorted market: The case of Brazil's retail sector. *Review of Income and Wealth 60*(3), 499–524.

Di Giovanni, J. and A. A. Levchenko (2013). Firm entry, trade, and welfare in zipf's world. *Journal of International Economics 89*(2), 283–296.

Di Giovanni, J., A. A. Levchenko, and R. Ranciere (2011). Power laws in firm size and openness to trade: Measurement and implications. *Journal of International Economics 85*(1), 42–52.

Edmond, C., V. Midrigan, and D. Y. Xu (2015). Competition, markups, and the gains from international trade. *American Economic Review 105*(10), 3183–3221.

Edmond, C., V. Midrigan, and D. Y. Xu (2022). How costly are markups? *Journal of Political Economy*.

Feenstra, R. C., R. Inklaar, and M. P. Timmer (2015). The next generation of the Penn World Table. *American Economic Review 105*(10), 3150–3182.

Fujiwara, Y., C. Di Guilmi, H. Aoyama, M. Gallegati, and W. Souma (2004). Do Pareto–Zipf and Gibrat laws hold true? an analysis with European firms. *Physica A: Statistical Mechanics and its Applications 335*(1-2), 197–216.

Gabaix, X. (2009). Power laws in economics and finance. *Annual Review of Economics 1*(1), 255–293.

Gabaix, X. (2016). Power laws in economics: An introduction. *Journal of Economic Perspectives 30*(1), 185–206.

Gabaix, X. and A. Landier (2008). Why has CEO pay increased so much? *The Quarterly Journal of Economics 123*(1), 49–100.

Gollin, D. (2002). Getting income shares right. *Journal of Political Economy 110*(2), 458–474.

Hall, R. E. and D. W. Jorgenson (1967). Tax policy and investment behavior. *The American Economic Review 57*(3), 391–414.

Hansen, B. E. (2020). *Econometrics*.

Hsieh, C.-T. and P. J. Klenow (2009). Misallocation and manufacturing TFP in China and India. *The Quarterly Journal of Economics 124*(4), 1403–1448.

Jones, C. I. (2016). The facts of economic growth. In J. B. Taylor and H. Uhlig (Eds.), *Handbook of Macroeconomics*, Volume 2, Chapter 1, pp. 3–69. Elsevier.

Levinsohn, J. and A. Petrin (2003). Estimating production functions using inputs to control for unobservables. *The Review of Economic Studies 70*(2), 317–341.

Luttmer, E. G. J. (2007). Selection, growth, and the size distribution of firms. *The Quarterly Journal of Economics 122*(3), 1103–1144.

Martinez, T. R. and T. T. O. Santos (2024). Revisiting the facts of economic growth: insights from assessing misallocation over 70 years for up to 100 countries. *Central Bank of Brazil Working Paper Series* (603).

Melitz, M. J. (2003). The impact of trade on intra-industry reallocations and aggregate industry productivity. *Econometrica 71*(6), 1695–1725.

Okuyama, K., M. Takayasu, and H. Takayasu (1999). Zipf's law in income distribution of companies. *Physica A: Statistical Mechanics and its Applications 269*(1), 125–131.

Olley, S. and A. Pakes (1996). The dynamics of productivity in the telecommunications equipment industry. *Econometrica 64*(6), 1263–1297.

Peters, M. (2020). Heterogeneous markups, growth, and endogenous misallocation. *Econometrica 88*(5), 2037–2073.

Petrin, A. and J. Levinsohn (2012). Measuring aggregate productivity growth using plant-level data. *The Rand Journal of Economics 43*(4), 705–725.

Restuccia, D. and R. Rogerson (2008). Policy distortions and aggregate productivity with heterogeneous establishments. *Review of Economic Dynamics 11*(4), 707–720.

Restuccia, D. and R. Rogerson (2013). Misallocation and productivity. *Review of Economic Dynamics 16*(1), 1–10.

Santos, T. T. O. (2020). A general characterization of the capital cost and the natural interest rate: an application for Brazil. *Central Bank of Brazil Working Paper Series* (524).

Santos, T. T. O. and D. O. Cajueiro (2024). Zipf's law in the distribution of Brazilian firm size. *arXiv preprint arXiv:2409.09470*.

Souza Júnior, J. R. d. C. and F. M. Cornelio (2020). Estoque de capital fixo no Brasil: séries desagregadas anuais, trimestrais e mensais. *Ipea Working Paper* (2580).

Syverson, C. (2011). What determines productivity? *Journal of Economic Literature 49*(2), 326–365.

Syverson, C. (2019). Macroeconomics and market power: Context, implications, and open questions. *Journal of Economic Perspectives 33*(3), 23–43.

Vasconcelos, R. (2017). Misallocation in the Brazilian manufacturing sector. *Brazilian Review of Econometrics 37*(2), 191–232.

Wang, O. and I. Werning (2022). Dynamic oligopoly and price stickiness. *American Economic Review 112*(8), 2815–49.